PROVENANCE ANALYSIS AND DEPOSITIONAL SYSTEM OF THE LATE QUATERNARY SEDIMENT FROM THE GANGES-BRAHMAPUTRA (G-B) DELTA, BANGLADESH: APPLICATION OF STRONTIUM GEOCHEMISTRY

By

Mohammad Shahid Ullah

Thesis
Submitted to the Faculty of the
Graduate School of Vanderbilt University
in partial fulfillment of the requirements
for the degree of

MASTER OF SCIENCE

in

Earth and Environmental Sciences

December, 2010

Nashville, Tennessee

Approved:

Steven L. Goodbred

David Jon Furbish

To my mother, whose love and blessing are with
me in whatever I pursue

and

To my beloved wife, Farin, infinitely supportive

ACKNOWLEDGEMENT

I would like to extend sincere thanks to my advisor, Professor Steve Goodbred, for providing me the wonderful opportunity to pursue a M.S research at a prestigious university like Vanderbilt. I have greatly appreciated Steve's enthusiasm and unfailing encouragement during research period. He has been a fundamental contributor to my research and without his thoughtful insight, relevant advice and enthusiastic supervision, this thesis would not have been possible. He gives me a lifetime unforgettable memory of his benevolence, patience, intelligence, diligence and erudition.

I would also like to thank my committee member Prof. John Ayers and Prof. David Furbish for their good advice, invaluable insight and constructive criticism during my brief two years in the department. Special thanks to Prof. Calvin Miller at Vanderbilt University, who gave important comments on my thesis.

I would also like to thank Dr. Warner Cribb for his patience and assistance with XRF analyses at Middle Tennessee State University. Dr. Sunil Singh at Physical Research Laboratory, Ahmedabad, India is sincerely thanked for his support in isotopic analysis. I am also grateful to Dr. Sirazur Rahman Khan and Ahad Ali, Geological Survey of Bangladesh for supervising the field work in Bangladesh.

Finally, I wish to thank my mother, without whom I would not be the person I am and my wife, Farin, for being a constant source of happiness and encouragement, and so much more.

TABLE OF CONTENTS

LIST OF TABLES

LIST OF FIGURES

CHAPTER I

Introduction

1.1 Introduction

The Ganges and Brahmaputra Rivers both originate in the tectonically active Himalaya, but follow separate paths before joining in the Bengal Basin and discharging to the Bay of Bengal. From their source areas to the Bengal Basin, the rivers erode numerous geological formations of distinct rock types engendering the highest sediment discharge to the global ocean of any of the world's river systems (Milliman and Syvitski, 1992). At the continental margin, these two fluvial systems consequently formed more than 100,000 km^2 of riverine channel, floodplain and delta plain during the late Quaternary that comprise the modern Ganges-Brahmaputra (G-B) delta, considered the largest subaerial delta system in the world (Goodbred et al., 2003). Previous studies showed that most of the Late Quaternary Ganges sediments were derived from the crystalline rocks of the High Himalayas and the Lesser Himalayas (Singh, et al., 2008) and the Brahmaputra sediments were eroded from the Tethyan Himalaya and Tibetan Plateau with a major contribution from Higher Himalaya (Singh and Lanord, 2002; Singh, et al., 2006; Stewart et al., 2008). With variations in tectonics, climate and erosion, these two river systems might have avulsed and migrated considerably within the G-B delta causing shifting provenance sources throughout the Late Quaternary. Therefore, understanding river behavior is necessary for reconstructing the development of the G-B delta system during the Late Quaternary.

Several studies in the past have discussed preliminary concepts of G-B delta stratigraphy and evolution (Goodbred and Kuehl, 2000b; Goodbred et al., 2003; Heroy et al., 2003; Allison et al.,2003). Several studies have also described the distribution of erosion in the Brahmaputra and Ganges watershed in the Late Quaternary from isotopic compositions of stream sediments (Derry

and France-Lanord, 1997; Galy and France-Lanord, 2001). However, much work remains for further unraveling the processes and mechanisms responsible for the depositional history in the G-B delta in relation to river position and sediment provenance. This study presents a detailed analysis of provenance, geochemical nature and the fluvial depositional system for sediment comprising the G-B delta aiming a better understanding of the late Quaternary fluvial dynamics and the consequent shifting provenance sources. Specifically, this study will evaluate the geochemical and stratigraphic record of four new well cores collected from the western portion of the G-B delta, Bangladesh with the aim of constraining the Ganges River end-member.

1.2 Study Area and Approach

The study area is a part of the upper deltaic plain of the G-B delta located at the southwestern part of Bangladesh (fig. 1.1). Bangladesh, which is one of the most densely populated regions of the world, is exposed to frequent flooding as a majority of its land lies only a few meters above sea-level. Therefore, it is critical to understand prior response of the delta system during changes in climate and sediment flux throughout the Late Quaternary. The Holocene development of the delta starts around 11,000 yr B.P, two to three thousand years earlier than other major delta systems. At present, the upper delta is inactive with virtually no sedimentation due to the absence of any major river system. However, the abundant presence of old natural levees, wide interdistributary floodplains, cut-off meander channels, oxbow lakes, and numerous point bars indicate the earlier presence of a major river system.

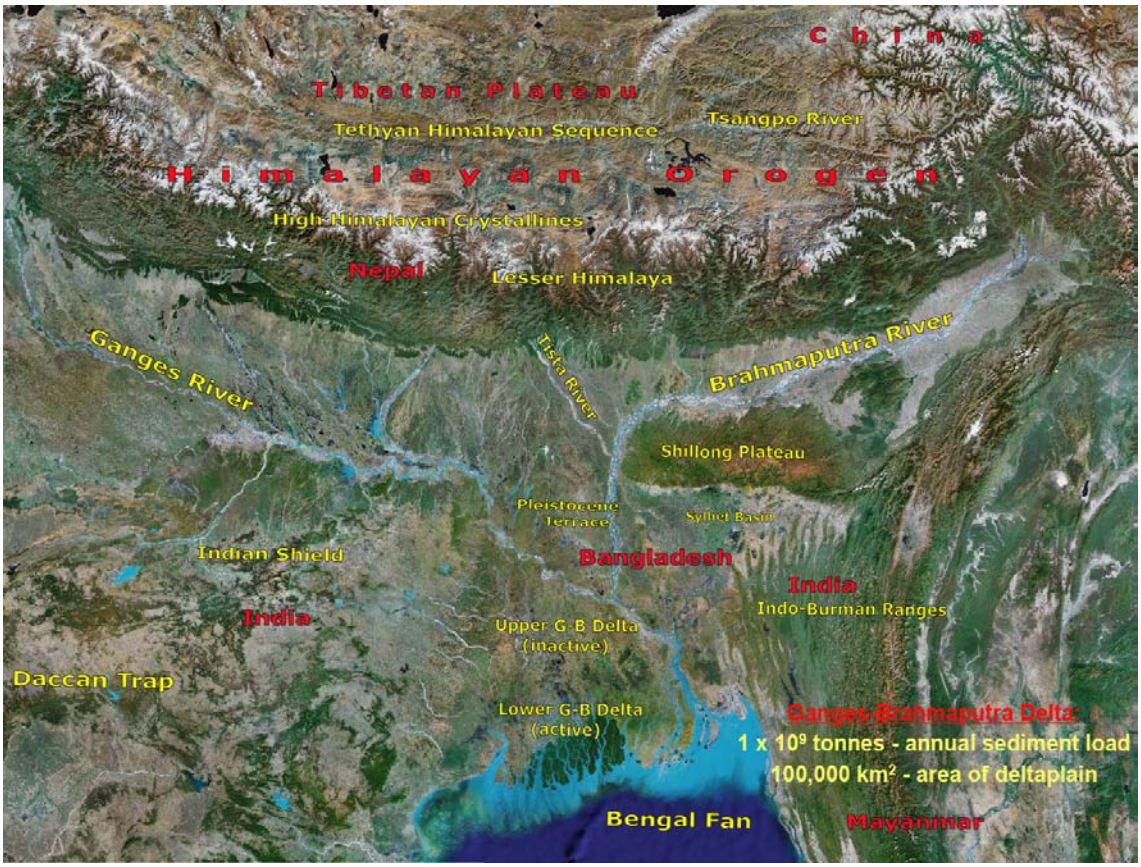

Figure 1.1: Regional map of the G-B delta along with the major tectonic provinces in the Indian subcontinent.

The provenance study in this research is pursued using the total strontium (Sr) concentration, $^{86}Sr/^{87}Sr$ ratios and the Nd isotopic ratios of the sediments collected at different depths from various parts of the G-B delta. Although both the Ganga and Brahmaputra Rivers drain the Himalayan orogen, local lithologies vary considerably and their $^{87}Sr/^{86}Sr$ isotopic ratio, as well as Sr concentration, are quite different (fig. 1.2). Therefore, Sr can be an effective means to trace sediment provenance in the Bengal Fan (Lanord et al., 1993). In a recent study, Singh et al. (2008) demonstrated that the Sr and Nd isotope compositions of the Higher and Lesser Himalaya are quite distinct and can be used to trace variations in the relative proportion of sediments deposited in the Ganga plain, India. Similar studies in the Bay of Bengal (Ahmad et al.,

2005; France-Lanord et al., 1993) showed that Sr isotope compositions of the silicate fraction of sediments are also useful to assess temporal variations in provenance.

Unfortunately much less is known about the Sr content and $^{87}Sr/^{86}Sr$ isotopic ratios of the upper and middle G-B delta sediments and their provenance. Therefore, in this study, Nd and $^{87}Sr/^{86}Sr$ isotopic ratios and Sr concentrations of sediment from four boreholes in the G-B delta will be used to investigate temporal variations in their provenance and to reconstruct the changing inputs of these two river systems based on their geochemical characteristics.

Sediment samples for this research were collected from four 50 to 100 m long boreholes, using local drilling method. These sediments store a high-resolution record of fluvial sediment eroded from the Himalayan catchment, which is controlled by various forcing mechanisms such as climate and tectonics. Because primary minerals dominate sediments collected from these boreholes, their trace element composition should reflect the original trace element signature of the source rock. Therefore, we can expect that the sediment samples, which are actually complex mixtures of eroded material transported by these two rivers from the Himalaya, should represent similar range in Sr concentration and $^{87}Sr/^{86}Sr$ values. To reconstruct the history and evolution of the entire G-B delta, results from this study are combined with data from previous work. A comparison of the stratigraphy and sedimentary records preserved in these boreholes gives us the complete picture of the late Quaternary delta formation.

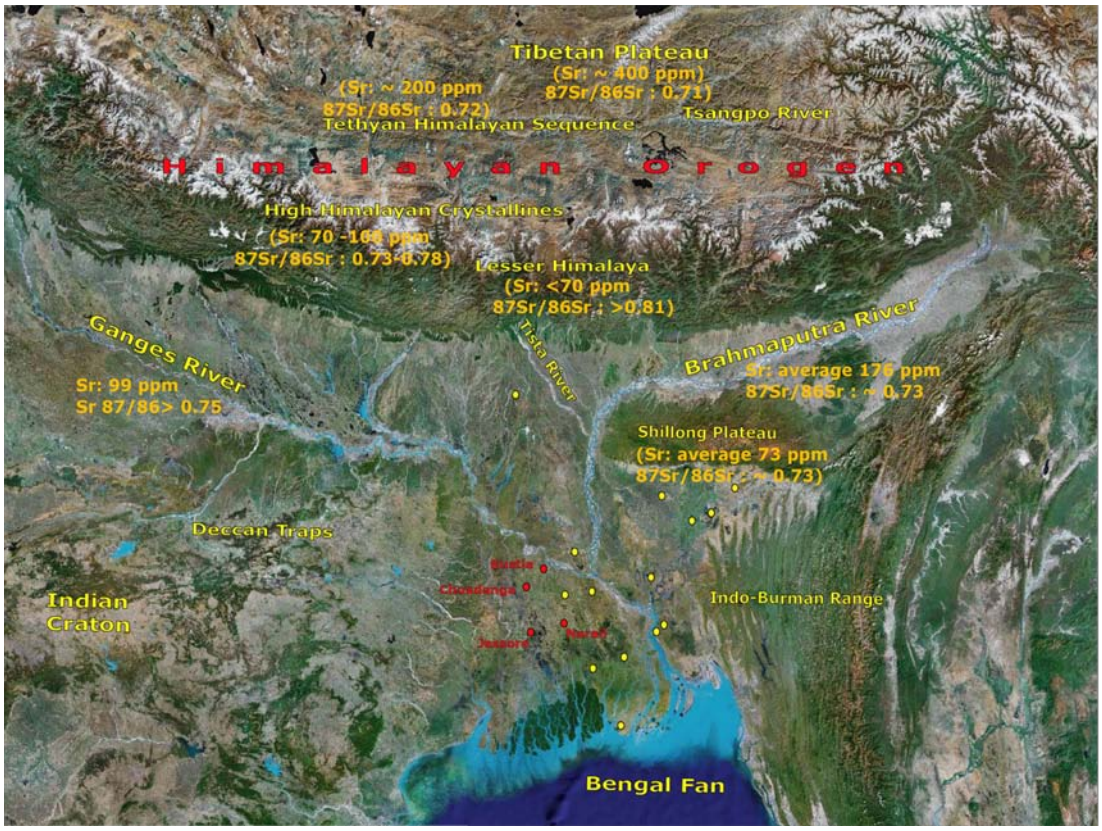

Figure 1.2: Approximate locations of the all-available boreholes used in the present study in relation to the Ganges and Brahmaputra Rivers and the G-B delta. Red dots on the figure represent boreholes drilled for the present study; yellow dots represent the previous boreholes. Also, note the Sr concentrations and isotopic ratios of different Himalayan provinces and the Tibetan plateau.

1.3 Background

1.3.1 Ganges Drainage System

The Ganga supplies ~500–1000 × 10^6 tons of sediments annually to the Bay of Bengal, which derive mostly by its northern tributaries coming out from the Higher and from Lesser Himalaya (Milliman and Syvistki, 1992). According to the calculations by Singh et al (2008), less than 10 percent of the Ganges sediments entering the G-B delta are derived from the Indian Craton by the southern tributaries. Because of their negligible contribution, the Sr concentrations

and the isotopic ratios of the southern tributaries were not considered in the present study. Among the northern tributaries Yamuna, Ghagra, Gandak and Kosi are the major ones responsible for bulk of the sediment that are coming out from the Himalaya in addition to the Ganges mainstream (Singh et al, 2008). Although the sediment of these four tributaries and the Ganges main stem have different Sr concentrations and isotopic values, they were not considered separately in this study but are considered as an averaged bulk signature for sediment transported into the G-B delta in Bangladesh.

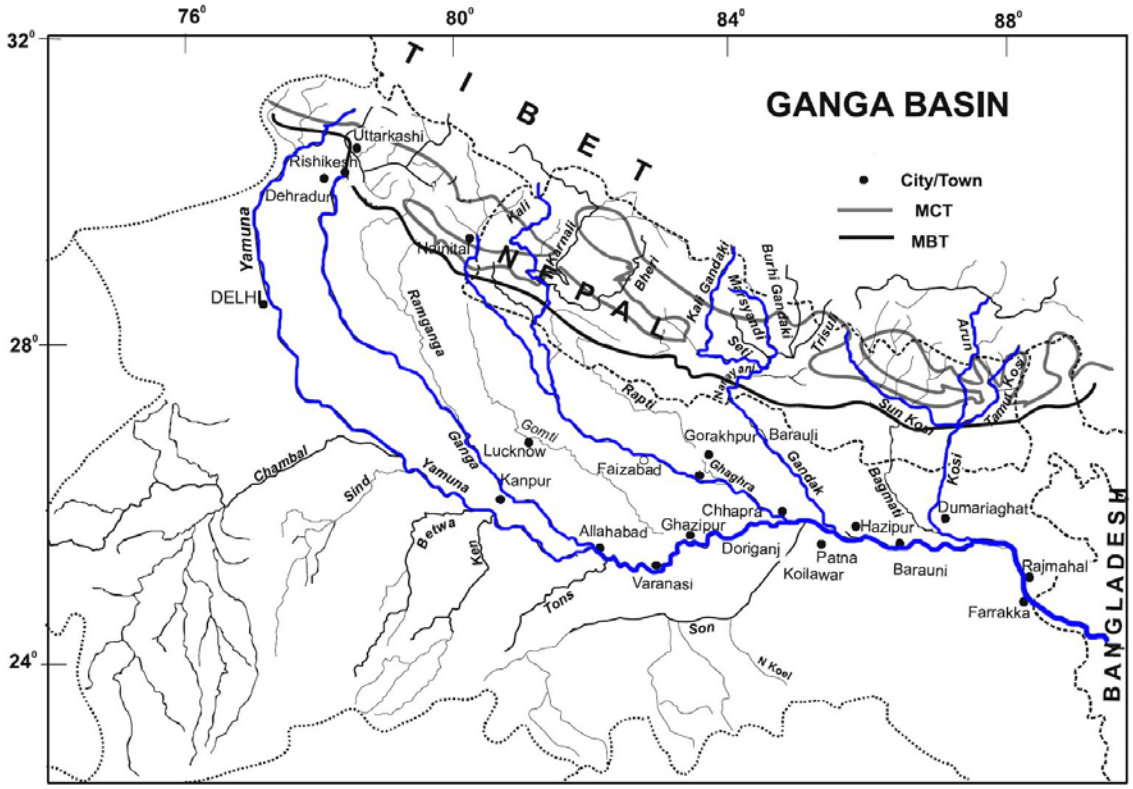

Figure 1.3: Map of the entire Ganges drainage system from Delhi in the west to Farrakka in the east. The drainage marked with blue represents the main Ganges stream and its four major tributaries, which are responsible for more than 90 percent sediment coming out from the Himalaya (Singh et al, 2008).

1.3.2 Brahmaputra Drainage System

Headwaters of the mighty Brahmaputra River originate in the north-central Himalayas, over 5,300 meters above sea level, and flows west to east across the southern part of the Tibetan Plateau and along the backside of the High Himalaya. After flowing east for >1200 km along the Tibet-Tsangpo suture zone, the Yarlung Tsangpo river towers over the Tsangpo gorge, which curves from the west, through the north, and then turns to the south at and through the Namche Barwa–Gyala Peri massif in the Eastern Syntaxis that rise to over 7000 meters (Finnegan et al., 2008). According to Burg et al., 1997, Zeitler et al., 2006 and several other workers, the Namche Barwa–Gyala Peri massif has recently been undergoing active deformation and rapid unroofing for the past 10 m.y. Burg et al. (1997) also suggest that regional denudation driven by the incision of the Yarlung Tsangpo–Brahmaputra passively paced rock uplift thereby enabling nearly 30 km of rock uplift and exhumation since the late Miocene. Downstream from Arunachal Pradesh, India where it passes the eastern syntaxis of the Himalayan orogen and known as the "Dihang", the river becomes wider with a new name- “Brahmaputra”. Uplift of Shillong plateau during 9-15 m.y ago (Biswas et al., 2007) forced Brahmaputra to flow west along the north side before turning south into the Bengal basin and discharging into the Bay of Bengal.

In contrast to the majority of other Himalayan rivers with little source area on the Tibetan Plateau, the Tsangpo–Brahmaputra River transmits a huge volume of water from the Tibetan Plateau (Finnegan et al 2008). Therefore, it has been assumed that the Tibetan plateau and the Eastern syntaxis shares equally the dominant proportion of sediments transported to the Bengal Basin.

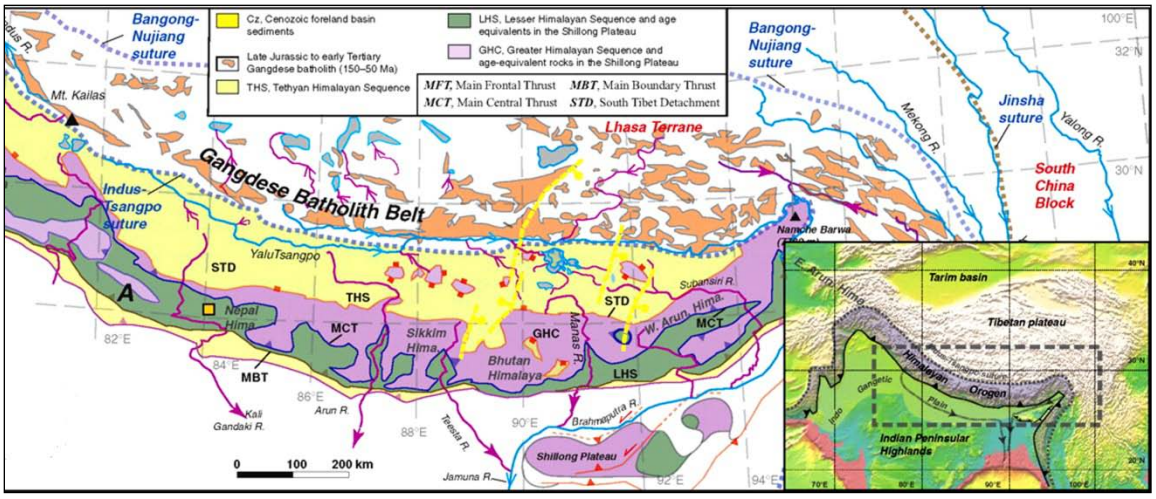

Figure 1.4: Map showing the entire Brahmaputra main stem and its tributaries draining through the Tibetan Plateau and along the backside of the High Himalaya. (Célérier et al., 2009)

1.3.2 Strontium Geochemistry of Himalayan Provinces and Rivers

Turekian and Kulp (1956) analyzed approximately 700 silicate rocks and 300 carbonate rocks taken from crust all over the world including Himalaya and showed that the difference in Sr concentrations relative to calcium content in granitic rocks. From their measurements they have shown that for an average Ca content of 0.6%, the Sr concentration is 100 ppm and for a Ca concentration of 1.9%, the Sr content is 440 ppm in the rock. This explains the wide range of Sr concentration values among the various provinces of Himalaya and Tibet as these provinces are formed of different rock types of different Ca content. Singh and Lanord (2002) found a range of 32 ppm to 428 ppm in total Sr concentrations and a range of 0.7053- 0.8250 in $^{87}Sr/^{86}Sr$ ratios recorded in sediment eroded from various formations in the Himalayas and Tibet. Moreover, they showed that the Sr contrast in sediments within main channel of the Brahmaputra at different localities in Tibet and the Himalayas is largely independent of SiO_2 content and concluded that this Sr contrast derives from source variability rather than a sorting or grain-size effect.

Segall and Kuehl, 1992 compiled at least 12 different lithological units in the Ganges and Brahmaputra drainage basins (see fig. 1.5), which are distributed among the four Himalayan

provinces and showed that the lithologies of the Himalaya provinces are quite different from the Tibetan plateau. The Tibetan Plateau mostly consists of Trans- Himalayan Plutonic Batholiths, which are young (Late Jurassic to Early Tertiary) granitic Batholiths (see fig. 1.4). On the other hand, the Tethyan Himalaya or the Tethyan Sedimentary Series is mostly sandstone, shale and limestone of Mesozoic age (see fig. 1.5). The Higher or Greater Himalaya is dominated by Precambrian metamorphics and younger felsic intrusions with a narrow sedimentary sequence of Cambrian sandstones, phyllites and dolomites. The Lesser Himalayan Sequence is mostly Precambrian metamorphics- schists, gneisses, quartzites and limestone (Segall and Kuehl, 1992).

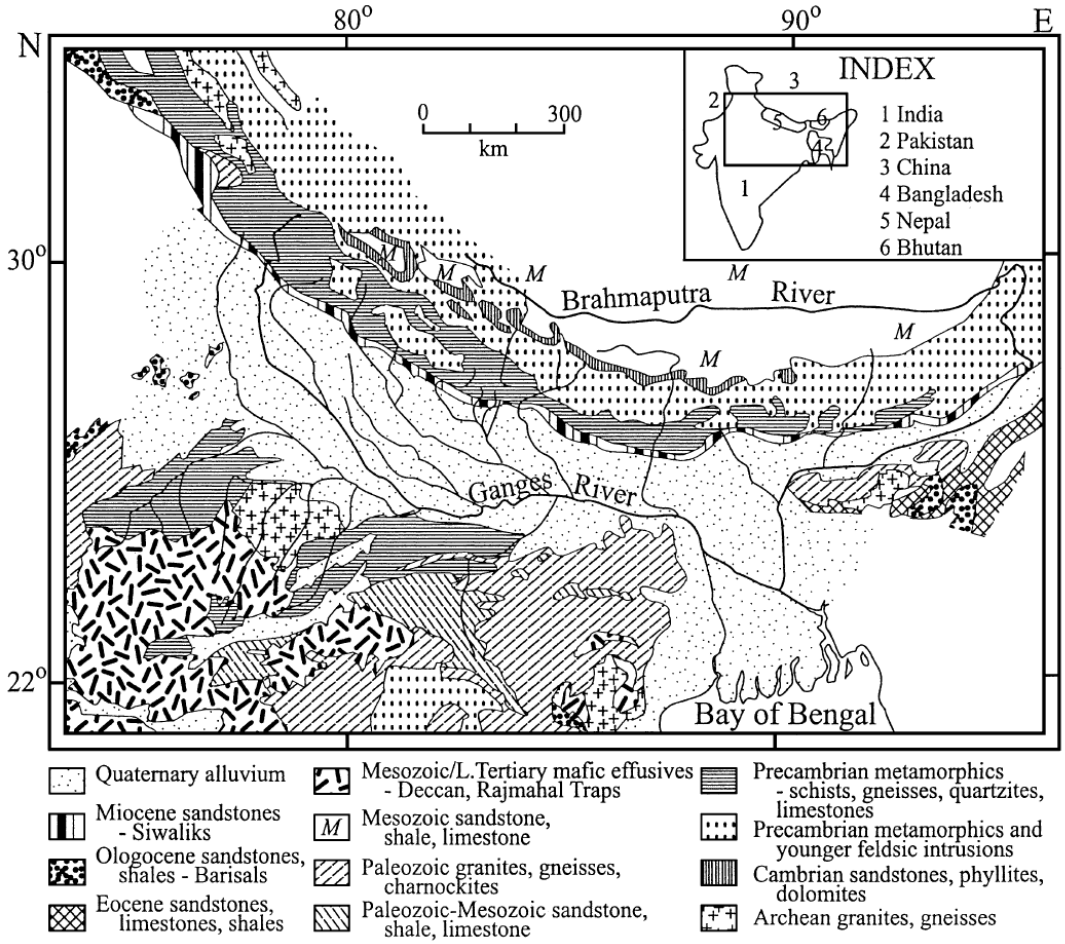

Figure 1.5: Geologic map of the Ganges and Brahmaputra drainage basins and surrounding areas. Unique lithologies drained by each river impart variations in Sr and Nd concentrations and isotope values (Segall and Kuehl, 1992).

As these various provinces of Himalaya and Tibet show a great variation in their lithology and rock type, their Sr concentrations and Sr and Nd isotopic ratios, also show distinct ranges of value (see the table below). High Sr concentrations are usually associated with low Sr isotopic ratios, such as, occurs for Tibetan Plateau sediment. The younger granitic intrusions in the Tibetan Plateau have a Sr concentration > 400 ppm. However, it has a very low $^{87}Sr/^{86}Sr$ ratio of 0.71. In contrast, the Lesser Himalayan rocks, which are mostly Precambrian Metamorphics, have average Sr concentration < 70 ppm and very high $^{87}Sr/^{86}Sr$ ratios of more than 0.81. This contrasting value of Sr concentrations and isotopic ratios is a useful tool for the provenance analysis of the G-B delta sediments as they preserve the geochemical signatures of their source areas in Himalaya and Tibet. These Sr values are also useful in differentiating the Ganges input from the Brahmaputra as they erode sediments from different provinces in Himalaya and Tibet.

Domain	**Sr Concentration**	**$^{87}Sr/^{86}Sr$**	**εNd**
Tibetan Plateau	Very high (average ~ 400 ppm)	Very low (average~ 0.71)	
Tethyan Himalayan Sequence/ Tibetan Sedimentary Series	High (average ~200 ppm)	Low (0.71-0.73)	-2 to -17
Higher or Greater Himalaya	Low (70-100 ppm)	Low - High (0.73-0.78)	-12 to – 18
Lesser Himalaya	Very low (average <70 ppm)	Very high (average > 0.81	< -23
Shillong Plateau	Very low (average~ 73 ppm)	Low (average ~0.73)	

Table 1: Sr concentrations and Sr and Nd isotopic ratios of Himalayan provinces and Tibetan and Shillong plateau (Compiled from Debon et al., 1986; Derry and France-Lanord, 1997; Galy et al., 1999; Singh and Lanord, 2002; Singh et al., 2006).

It is important to note that, Ganges has very little input from Tethyan Himalaya and no sediment input from the Tibetan Plateau (see figure 1.3),which in contrast are the two major source areas for the Brahmaputra river sediment. This largely explains why the Sr concentrations and isotopic compositions of silicate sediments eroded by the Brahmaputra and Ganges rivers exhibit large differences. Sediment eroded from the Brahmaputra watershed is much less radiogenic than Ganges sediments because of significant Sr contribution from Tibetan lithologies with low $^{87}Sr/^{86}Sr$ values (Derry and France-Lanord, 1997; Singh et al., 2006). Brahmaputra sediments typically have $^{87}Sr/^{86}Sr$ values in the range of 0.72 to 0.74, while Ganges sediments have significantly higher $^{87}Sr/^{86}Sr$ values approaching 0.80, because of sediment flux dominated by more radiogenic Himalayan lithologies.

Along its Tibetan reach, the Brahmaputra River transports sediment nearly equally derived from the Tibetan Plateau and the Tethyan Himalaya, with high Sr concentrations due to the concentrations from Tibet (Sr>400 ppm) and the Tethyan Himalayan (Sr ~ 200). However, the biggest share of Brahmaputra sediment reaching the G-B delta is coming from the Namche Barwa and Eastern Syntaxis where the river cuts the deepest canyon system on the earth. Near the Namche Barwa–Gyala Peri antiform, ^{10}Be-derived basin-averaged erosion rate was found as high as 4 mm/yr over a 3000 m range of mean relief, which is one of the highest on the present earth (Finnegan et al., 2008). The Namche Barwa peak falls within the Higher Himalaya provinces, which has low Sr concentrations of 70-100 ppm and high isotopic ratios of 0.73-0.78. Since more than 50% of the Brahmaputra fluvial load is supplied by this region, the Sr concentrations drops and the isotopic ratio increases through this region. After small sediment input from the Shillong Plateau, which has both low Sr concentration and isotopic ratio, the final average concentration and isotopic ratios of the fluvial load that is reaching G-B delta through Brahmaputra is 176 ppm and 0.74 respectively (Galy and Lanord,1999).

In contrast, more than 90 percent of the Ganges sediment is coming from the Higher or Greater Himalayan sequence, Lesser Himalayan sequence, Himalayan Foreland Basin sediment and the Quaternary alluviums (Wasson, 2003). Only less than 10 percent of the Ganges sediments are contributed from the Indian Craton by the southern tributaries of Ganges. Therefore, in this research it is assumed that the sediment contribution from the Indian Craton, and their Sr concentrations and isotopic values are not vital for a provenance analysis of Ganges sediment.

CHAPTER II

Methods

2.1 Field Work

Four borehole sites in the southwestern part of Bangladesh, near Jessore, Chuadanga, Kustia and Narail districts were selected for the sample collection in the present study (fig. 1.2). All of these borehole sites are located in a region that is south of the Ganges River and west of the Brahmaputra. The drill sites are separated by about 100 km, from Kustia at the north to Jessore at the south. In addition to the four boreholes collected for this study, data from other borehole locations are also used in the analyses.

A total of 192 samples were collected from the four boreholes starting from the surface to a maximum depth of 97 m with a sampling interval of 1.6 meter. Local chopping technique for tube well installation was used to drill the borehole, which is an inexpensive and time efficient method of collecting continuous samples. Each sample from the borehole represents a continuous sampling from a 1.6 m interval. However, as these are cutting samples that are circulated by water from the bottom of the borehole, no sedimentary structures was preserved. Samples were described in the field before being air-dried and packaged and shipped from Bangladesh to Vanderbilt University for laboratory analysis.

2.2 Laboratory work

2.2.1 Grain size analysis

147 sand samples out of 192 were analyzed for their grain-size distribution using a Malvern Mastersizer 2000 laser-diffraction particle-size analyzer. This instrument generates grain

size data from an average of three consecutive grain size analyses for each sample. Before the grain size analysis, the samples were sieved to remove the sediment fraction less than 63 um. Only the sand-sized fractions were used in the present study because it is more robust geochemical provenance indicator compared to silt and clay-sized fractions (Pate, 2008) because sand is deposited close to the river channel, where silts and clays can be transported considerable distances from the channel from which they originated.

2.2.2. Magnetic susceptibility

Magnetic susceptibility measurement of the samples was performed using a GeoTek Multi- Sensor Core Logger (MSCL) that is equipped with magnetic susceptibility measurement system. The magnetic susceptibility measurements were done on all 192 sand and mud samples. Each sample was measured twice and the results averaged.

Magnetic susceptibility represents the degree of magnetization of a material in response to an external magnetic field. The magnetic susceptibility of sediment largely depends on the presence of ferromagnetic and anti-ferromagnetic minerals. Very high concentration of other para-magnetic and dia-magnetic minerals can also cause higher magnetic susceptibility value (Sangode et al., 2007). Verosub and Roberts (1995) showed that magnetic susceptibility of sedimentary deposits could be successfully applied as a reliable indicator of changing depositional processes, climate change, sediment provenance, and post-depositional alteration. Magnetic minerals in sediment reflect source material, erosion, transport, depositional processes, depositional components, and post-depositional processes, which vary according to climate and tectonics (Verosub and Roberts, 1995). Pate (2008) showed that magnetic susceptibility might be useful in detecting shifts in monsoonal regimes within the stratigraphic record in the G-B delta. He found high magnetic susceptibility values occur in weathered sediments from the Pleistocene lowstand exposure surface. He also showed that sediments with unusually high magnetic

susceptibility peaks typically exhibit distinctly different elemental composition compared to sediments with background magnetic susceptibility values.

2.2.3 Elemental analysis

Approximately 84 samples from seven boreholes were analyzed for their major and trace elements content in this research. Other than the four boreholes, which were drilled for this research, sediment samples from three pre-existing boreholes were also measured for their major and trace element content. In addition, major and trace elemental data from few previous boreholes were recalibrated in this research.

Elemental analysis was primarily performed at Middle Tennessee State University using an Oxford Instruments MDX 1080+ multi-dispersive X-ray fluorescence spectrometer, in which a pressed powder pellet is analyzed directly for 30 elements. Major element results were normalized to 100% .The Ganga river sediment are reported to contain several percent carbonate (Heroy et al., 2003). Therefore, the following procedure was used to decarbonate the sediment samples during the sample preparation for XRF analysis.

Samples were first combusted at 600^0C for 72 hours in a muffle furnace and then treated with a10% HCl leach to remove carbonate material. Samples that reacted strongly to the HCL leach were noted to contain a significant fraction of carbonate material. Following an acetic acid leach, samples were rinsed 3 times with deionized water to remove excess HCl. Then the samples were dried before crushing into a fine powder using an alumina ceramic shatterbox. Finally, samples were pressed into pellets for XRF analysis using a hydraulic press set at 11,000 psi for 15 minutes. Major and minor elemental analyses were performed for each pelleted sample. Results were calibrated to a composite curve based on nine known standards.

2.2.4 Isotopic analysis

Sr and Nd isotopic measurements of 16 samples were performed by Dr. Sunil Singh at the Physical Research Laboratory, Ahmedabad, India using an Isoprobe –T Thermal Ionization Mass Spectrometer. Isotopic analyses were done using the same crushed sample pellets prepared for the XRF analysis.

CHAPTER III

Results

3.1 Borehole Lithology

Except the Jessore borehole, which contained only Holocene sediments the other three boreholes in the study area consist both of Pleistocene and Holocene deposits and their margin were identified in the field by the abrupt change in lithology from loose gray silty sand to stiff brown clay. McArthur, et al., 2004 and several other workers also found this impermeable brown clay in southern West Bengal, India and interpreted it as a local representation of a basin-wide low stand surface. With a few exceptions, most samples are strongly dominated by primary minerals such as quartz, feldspar, micas and the clay minerals. Only a few samples suggested significant sorting by transport and deposition processes where mica and heavy mineral intervals were observed. In the field, lithostratigraphic boundaries were usually recognized by changes of lithology and physical characteristics of the sediments, such as color and texture. In addition, the grain size data were used to establish the lithostratigraphic boundaries more precisely. In some cases, the gradational boundary between these units made it difficult to identify any lithostratigraphic boundaries.

Both of the Holocene and Pleistocene deposits are composed of different clay, silt and sand units. However, the Pleistocene sediments are comparatively coarser than those of the Holocene. Surface deposits (soil) within the upper meter or two range from dark olive gray sandy silt to dark grayish brown massive silt. In some places, it was moist and sticky, with few patches of yellowish brown color. However, in most of the cases it was loose and friable. Huge roots and rootlets were present in the soil horizons in most cases. A few burrows and incipient nodules were also found. Distinct changes in lithology between these surface soils and the underlying unit

was observed in all of the boreholes. Clayey silts and sands were often found interbedded in these four boreholes where clay bands were usually 5-8 cm thick. The clayey silts are dark olive gray colored, massive, sometimes moist, somewhat stiff and moderately sticky. The sand deposits are dark olive gray to greenish gray colored and massive. Quartz content ranges between 78-91% with significant amount of stained and fresh quartz grains at some depths. Very few shell materials with their fragments of molluscan fauna are present. Decomposed vegetal matter and plant fragments were also found at some depths.

Samples collected at depths of 26- 27 meters in Kustia, 42- 43 m in Chuadanga and 47-48 m in Narail are distinctly stiff, orange to brown colored relative to other samples and are interpreted to be Pleistocene sediment near the Holocene-Pleistocene boundary. However, this type of surface was not found in Jessore where the borehole probably hit an incised paleochannel, which might have eroded the previous Pleistocene surface. Several workers for example Goodbred and Kuehl (2000), McArthur, et al. (2004) interpreted this stiff, oxidized orange to brown colored sediment as weathered paleosols formed during Late Pleistocene lowstand of sea level. They also noted that this paleosol horizon is present throughout the Bengal Basin and generally divides the Quaternary stratigraphy into Holocene and Pleistocene sequences.

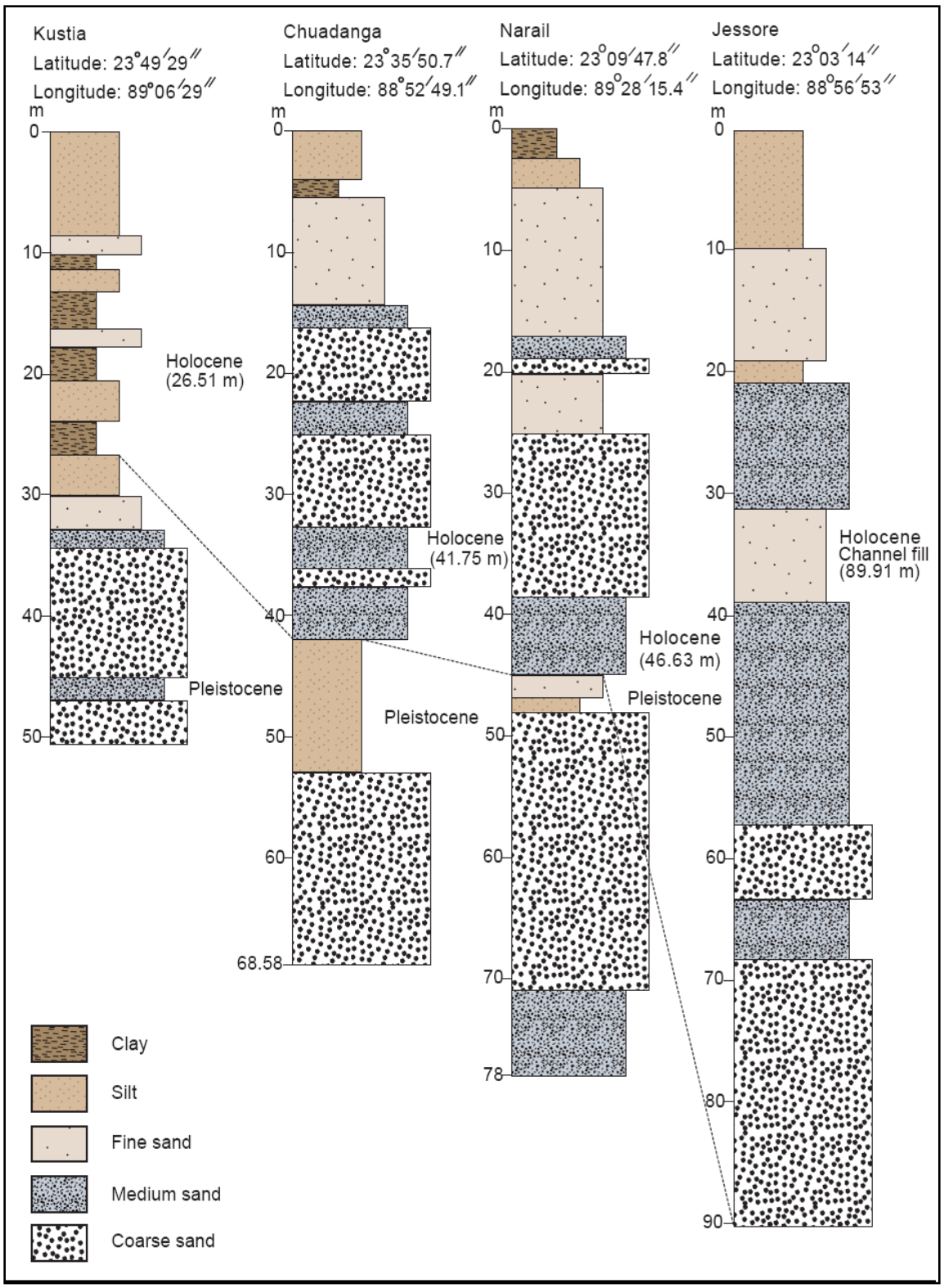

Figure 3.1: Litholog of the boreholes used in this research. Note that the dashed line represents the surface distinguishing the Holocene deposits with the Pleistocene.

3.2 Grain Size

Down-core grain-size data for the sand fraction was collected from the four boreholes to determine the geologic significance of certain grain size parameters and to study the behavior of the size fractions with river shifting and associated change in the energy of transport. Grain size data shows overall fining upward trends in each of these four boreholes (fig.3.2). However, within the sand fractions, there is alternating coarsening upward and fining upward trend, which might indicates several cycles of river shifting or bar formation in these borehole sites since the late Quaternary. The Jessore borehole, which consists of entire 90 m of Holocene sediment, shows two distinct coarsening upward sequences interspersed with two distinct fining upward grain size trends. In the other three boreholes, the Pleistocene sediments distinctly show coarsening upward trend up to the Pleistocene-Holocene boundary and then the grain size become finer in the early Holocene deposits.

Among the four boreholes, the Kustia sediments are comparatively finer with average 2.5% clay and 20% silt. The measured 20 samples from the Kustia borehole show a volume weighted mean grain size ranging from 3.9 μm to 590 μm. The Chuadanga sediments are comparatively coarser than the Kustia with higher sand fraction (> 89%) and lesser silt and clay fraction (> 10% and <1% respectively). The measured 37 samples from the Chuadanga borehole show a volume weighted mean grain size ranging from 22 μm to 603 μm. The samples from Narail and Jessore borehole are comparatively much coarser than the Kustia and Chuadanga samples with an average sand fraction of >96% and >97% respectively. In Narail, the volume weighted mean grain size of 48 samples ranges from 46 μm to 585 μm whereas in Jessore the mean grain size of 51 samples ranges from 163 μm to 546 μm. The sand fraction from all four boreholes generally show a tri-modal mixture ranging from coarse/very coarse sand to fine sand/silt (see appendix).

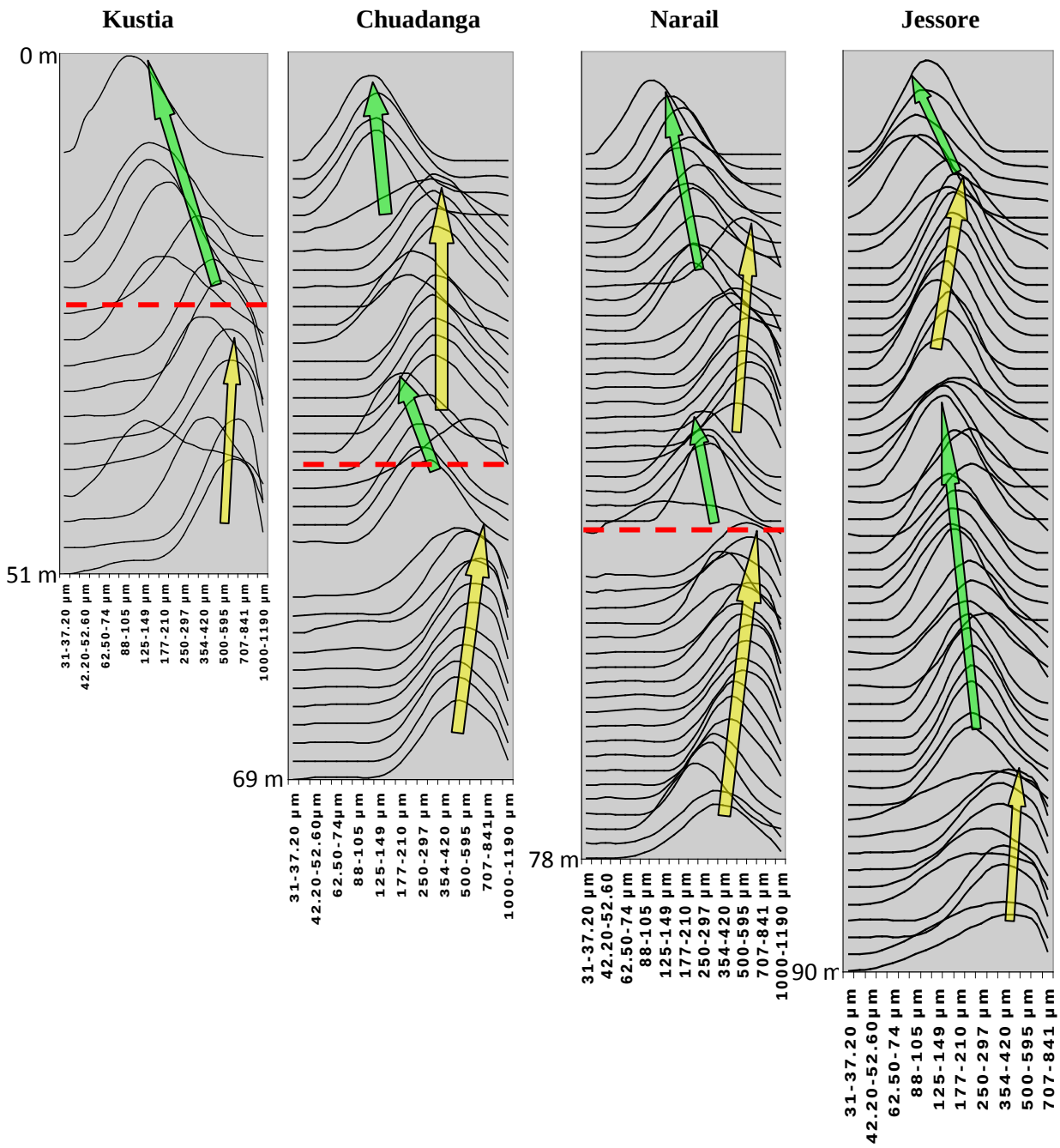

Figure 3.2: Grain size data showing overall fining upward trends in the studied four boreholes. Also, note the alternating coarsening upward (yellow arrow) and the fining upward trend (green arrow). Individual curve in each of these trends represents the grain size distribution in a single sample. Red dashed line represents the Holocene-Pleistocene boundary.

3.3 Magnetic Susceptibility

Down borehole MS trends in borehole sediment show a wide range of MS values from 0 to 180 SI. There are discernible variations in color or lithology among the sediment of high and low magnetic susceptibility in Kustia. However, the magnetic susceptibility values varies from >180 SI to <50 SI within a single lithological unit of same lithology or grain size as seen in the other three boreholes.

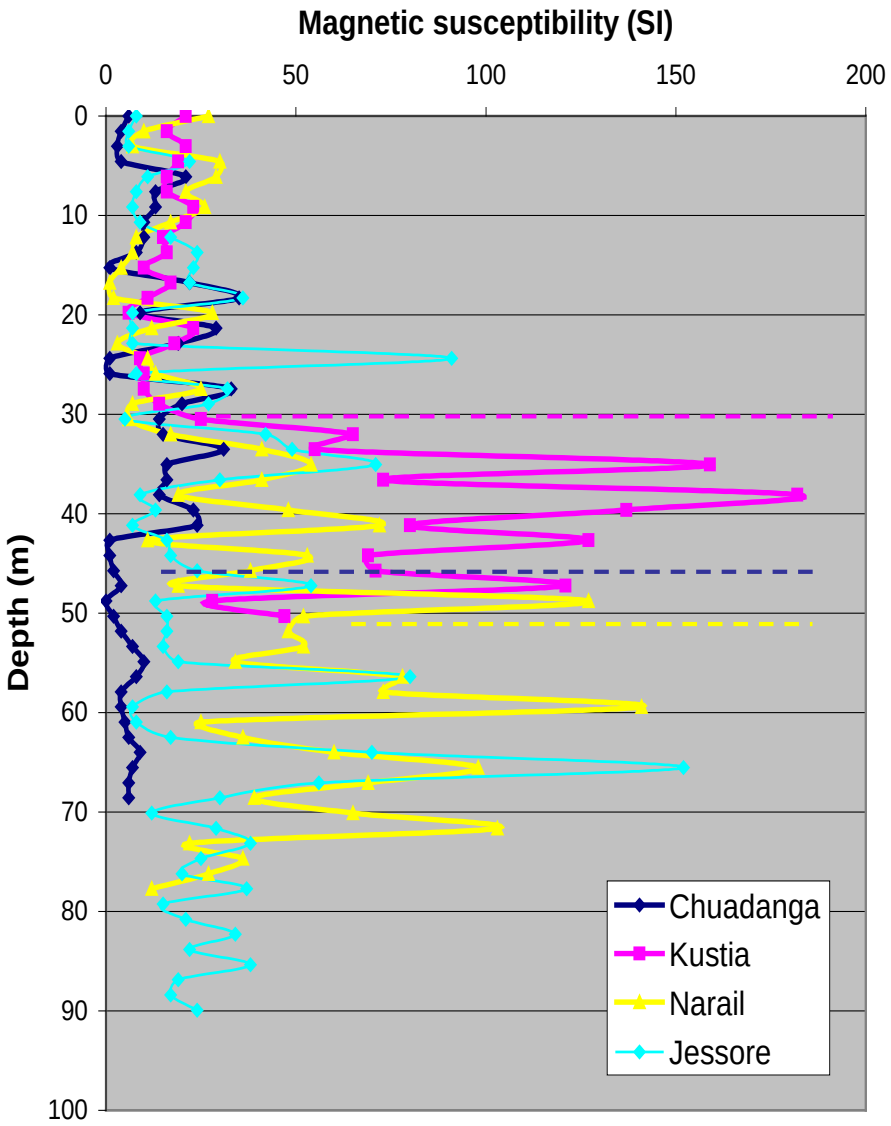

Figure 3.3: Down borehole magnetic susceptibility trends in the studied four boreholes. Note that the dashed lines represent the Pleistocene –Holocene boundary in the respective borehole.

The Holocene sediment usually shows a lower magnetic susceptibility values than the Pleistocene sediment. The only exception is Chuadanga where there is a sharp decrease of magnetic susceptibility values below the Holocene-Pleistocene boundary. With few exceptions, the Holocene sediments usually have a magnetic susceptibility value less than 50 SI. Whereas the magnetic susceptibility values for the Pleistocene sediment are as high as 180 SI. The magnetic susceptibility values show a weak positive correlation with grain size except Kustia where it shows a strong correlation.

3.4 Carbonate Content

Except for Jessore, which has a 90-meter thick Holocene sequence, the carbonate content of the borehole sediments sharply decrease below the Holocene-Pleistocene boundary (fig. 3.5). As there is virtually no correlation between the carbonate content of the sediment and the lithology or grain size, the only factor besides weathering that can cause this change in carbonate content is provenance. However, relatively low weathering indices of the borehole sediments calculated from the major elements shows that majority of the borehole sediments are not weathered. Previous workers showed that the carbonate content does not exceed 0.6% in the Brahmaputra sediments whereas it is 4-7% in the Ganga (Singh and Lanord, 2002).

3.5 Facies Analysis

Down borehole changes in sediment grain size, color, organic material content and magnetic susceptibility were used to develop a sedimentary facies scheme for the borehole sediments. Four facies type were identified, which are described below. The stiff, reddish-yellow to yellowish-red highly weathered paleosols found in these boreholes were not considered in the facies analysis as they represent the Late Pleistocene lowstand (Goodbred and Kuehl, 2000) and are primarily used for stratigraphic interpretations.

3.5.1 Facies A: Gray to bluish gray mud to dark greenish gray silty clay, very sticky; very few mottling also seen. Few very hard and stiff chunks of clayey silt are found. A large amount of decomposed vegetal matter was found within this facies. Facies A usually has a very low magnetic susceptibility value (<10 S.I). Facies A is absent in Jessore and Narail borehole and mostly found in Kustia borehole (fig. 3.6). Where present, facies A is less than 5 m thick.

Interpretation: Facies A is interpreted as distal floodplain deposits commonly found throughout the G-B delta. The deposition of Facies A is associated with slack water or low energy deposition from overbank floodwaters at some distance from a channel. Goodbred and Kuehl (2000 b) in their work described the same facies as “Thin Mud”.

3.5.2 Facies B: Facies B comprises dark olive, gray clayey silt to light olive brown silty sand; massive, moist and slightly sticky with yellowish brown mottling . A few incipient soil concretions are also found. Facies B gradually merges with Facies C with depth. Decomposed organic matter was found in some cases. Magnetic susceptibility values usually varied from 10-25 in this facies. Except Narail, Facies B is common in the boreholes and the thickness varies from 2 - 18 meters. Facies B can be distinguished from Facies A by its generally lower clay fraction and higher silt and fine sand fraction.

Interpretation: Facies B is interpreted as levee or splay deposits, which is also a commonly found facies in the G-B delta. It is also a slow water deposition; but unlike Facies A, it is much closer to the channel thus the transport energy is slightly higher.

3.5.3 Facies C: These deposits are composed of dark olive gray fine to medium, massive, sub angular to sub rounded and moderately well sorted sand. The Facies C shows fining upward trends in the upper half of the sequence and coarsening upward trends in the lower halves. Thin and sticky clay bands of 5-10 cm thickness were sometimes found alternating with very fine sand at the top or bottom of Facies C indicating a gradual transition from the facies B. Sands in this facies composed mainly of quartz varies from 70-91%, black minerals varies from 5-20%, mica and others about 3-9%. The magnetic susceptibility value in Facies C is usually high (generally >25 S.I). Facies C is the most common and abundant facies in the studied four boreholes. It can be as thick as 35 meter as found in Jessore borehole (fig 3.4).

Interpretation: Facies C is interpreted as alluvial valley and river channel fill. Deposition of Facies C overlying multiple sequences of Facies B indicates successive channel migration and river avulsion during the Late Quaternary. Goodbred and Kuehl (2000a) described this facies as "Sand Facies".

3.5.4 Facies D: Greenish gray coarse – v. coarse sand with concentration of hard pebbles and granule; massive, angular. Large quartz grains, some with staining were seen. Partly decomposed wood fragments and organic matter are also found. The magnetic susceptibility usually shows very high values in facies D. Facies D was found at the middle or lower portion of the four boreholes. It differs with Facies C with the addition of large granules/pebble sized fragments (1-2 cm) scattered within coarse to very coarse sand.

Interpretation: Facies D is possibly interpreted as the product of high-energy floods or main channel fill during enhanced monsoon and lower sea level. Except Jessore, the Facies D is quite thin in the other three boreholes (< 3 meter), which might indicates that it is a product of event deposition.

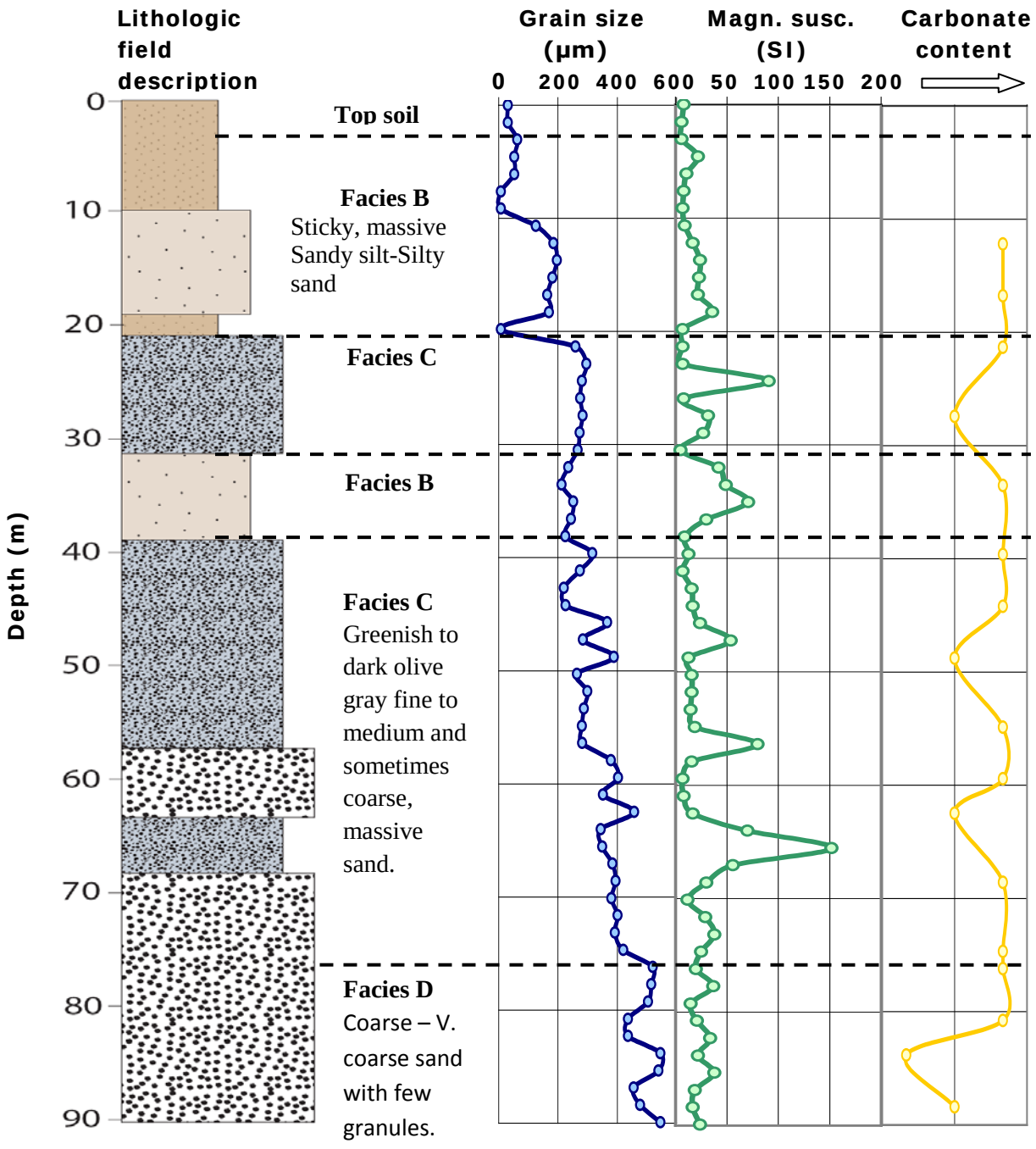

Figure 3.4: Compiled stratigraphy, grain size, magnetic susceptibility and facies for 90-meter thick Holocene sequence in Jessore.

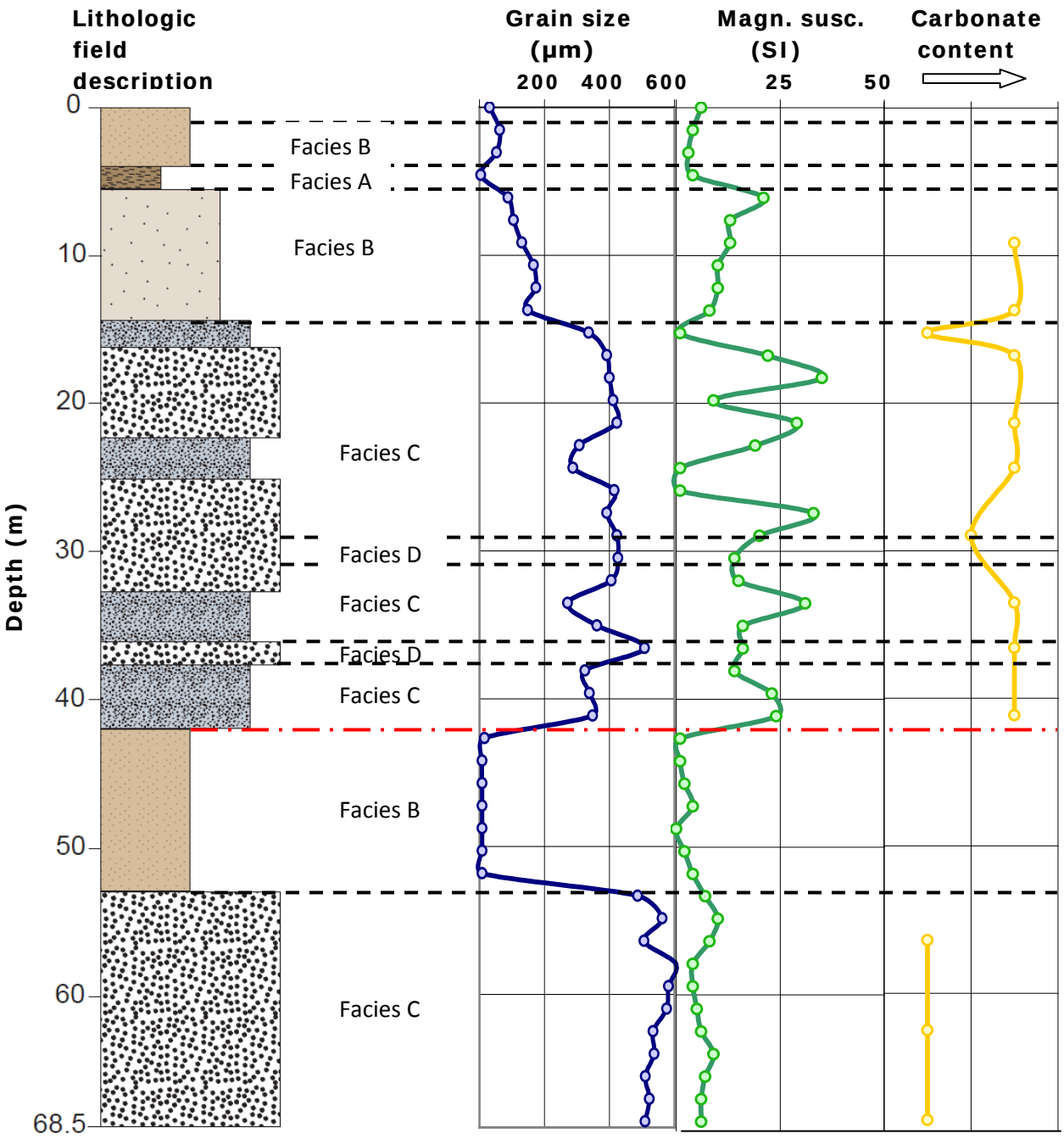

Figure 3.5: Compiled stratigraphy, grain size, magnetic susceptibility and facies for Chuadanga borehole.

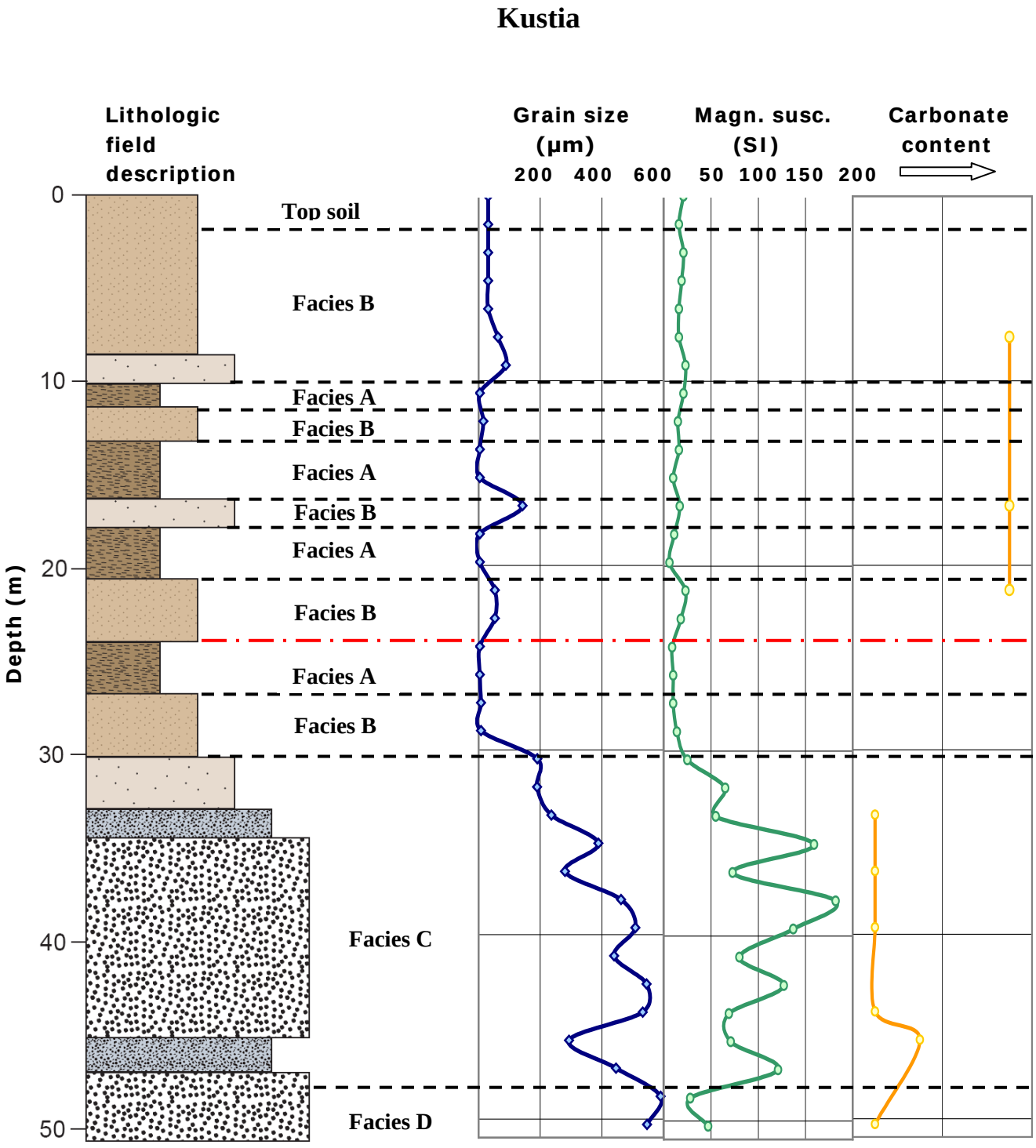

Figure 3.6: Compiled stratigraphy, grain size, magnetic susceptibility and facies for Kustia borehole.

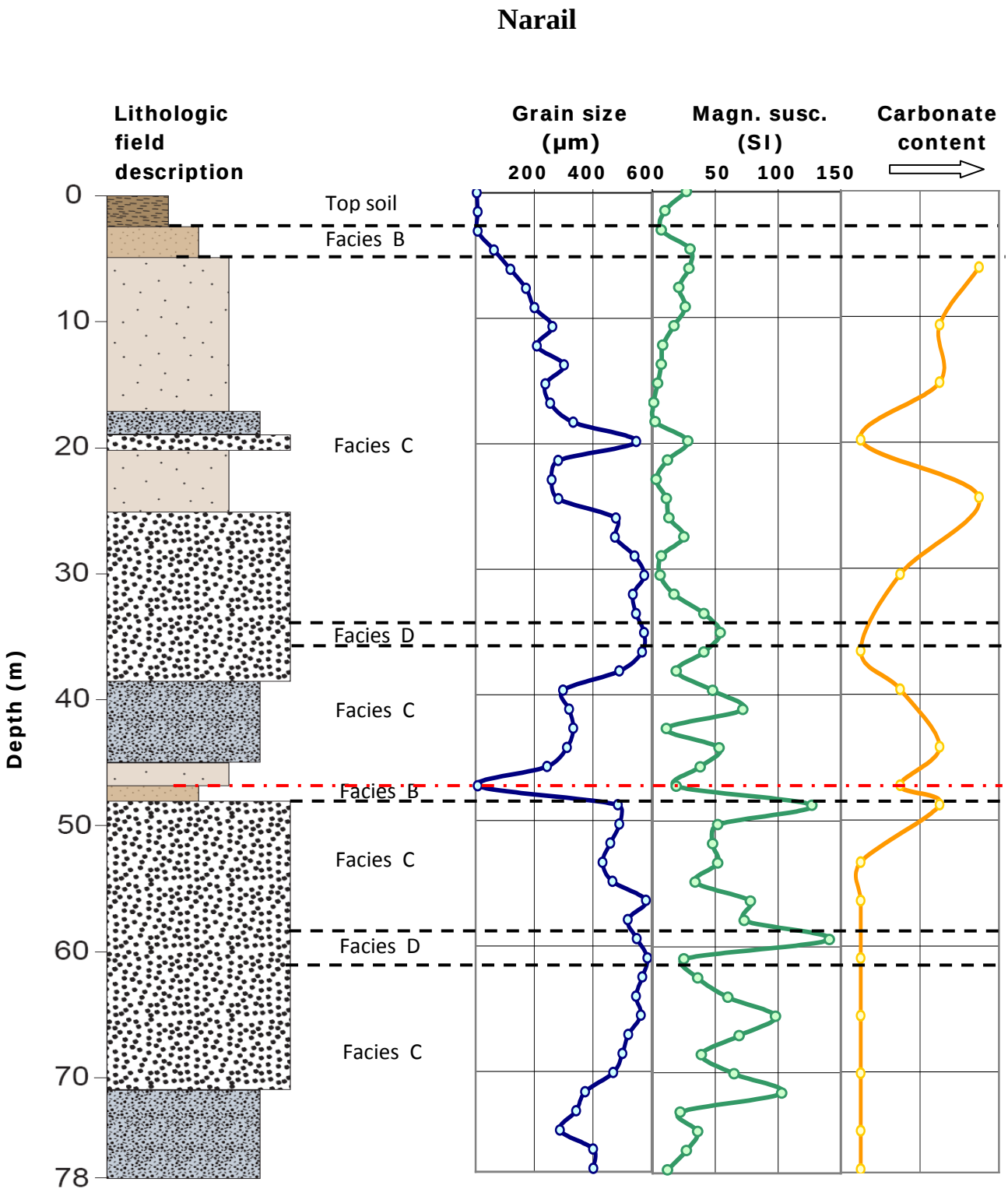

Figure 3.7: Compiled stratigraphy, grain size, magnetic susceptibility and facies for Narail borehole.

3.6 Elemental Analysis

A. Major elements: As a general observation, channel fill sediments (facies D) have higher SiO_2 content and lower Al_2O_3 content than the over bank fine-grained sediment. The borehole sediment also have lower Na and K contents compared to that of average continental crust because their sources are recycled crustal formations. They also have lower Ca and Mg and higher SiO_2 contents consistent with the relatively rare mafic, ultramafic and volcanic rocks in the catchment area of the Ganges and Brahmaputra River. The lower Ca, Na and K content are also common in the weathering horizons, which are typically enriched in Fe-oxides and depleted in Ca, Na and K (relative to Al).

Except few weathered horizon, there is little difference in major elemental composition between the Holocene and Pleistocene sediment. The only major element that shows a considerable difference between the Holocene and Pleistocene deposits is Ca. CaO content in most of the Pleistocene samples is almost 1.5 to 2 times higher than the Holocene (fig. 3.8).

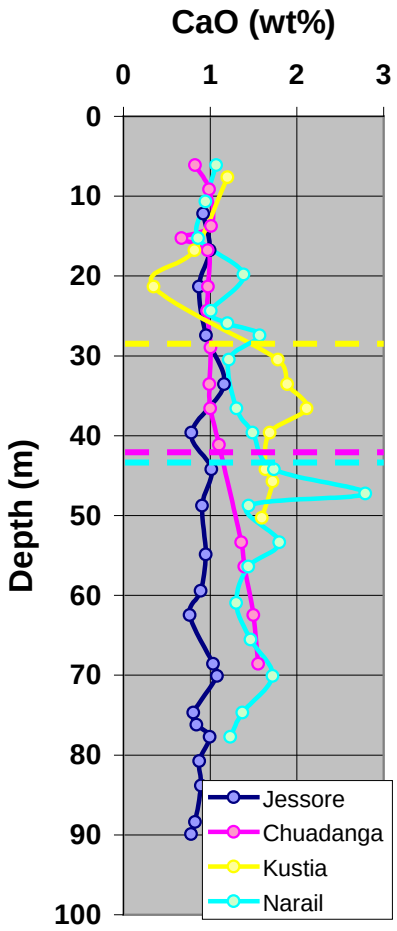

Figure 3.8: Down borehole CaO concentration showing an increase in Pleistocene sediments.

B. Trace elements: There are a number of trace elements that were detected from the elemental analysis by XRF, including Ba, Rb, Sr, Zr, Y, Nd, Zn, Pb, Th, Nb, Cu and U. Among these, Sr is the only trace element that shows distinctly different concentrations between the Holocene and Pleistocene sediment. Other than the Jessore borehole sediment that consists of a 90 m thick Holocene sequence, Sr concentrations increase from 90- 100 ppm to 150 ppm across the Holocene-Pleistocene boundary in Kustia and Chuadanga.

Among the trace elements, Rb, Y and Nb concentrations correlate throughout the borehole. Rb concentrations generally increase with a similar increase in Y and Nb. However, Sr concentrations do not correlate with Y and Nb, but is negatively correlated with Rb concentration. The Holocene sediments have a higher Rb concentration than the Sr, but below the Pleistocene surface, the Sr concentrations exceed the Rb concentration. The sharp increase of the Y and Nb values and the associated decrease in the Rb concentration at 45 meter in Jessore is may be due to the presence of a weathered layer indicated by a M.S. peak. The high values of Y, Nb and Rb associated with the low values of Sr might indicate a Lesser Himalayan input by an Eastern Himalayan river. The presence of a gravel bed at that depth also supports this idea. In Narail, a sudden increase of Rb, Y and Nb values between 20 and 25 meter and then a subsequent decrease might also indicate a provenance change, as there is no noticeable change in M.S values at that depth.

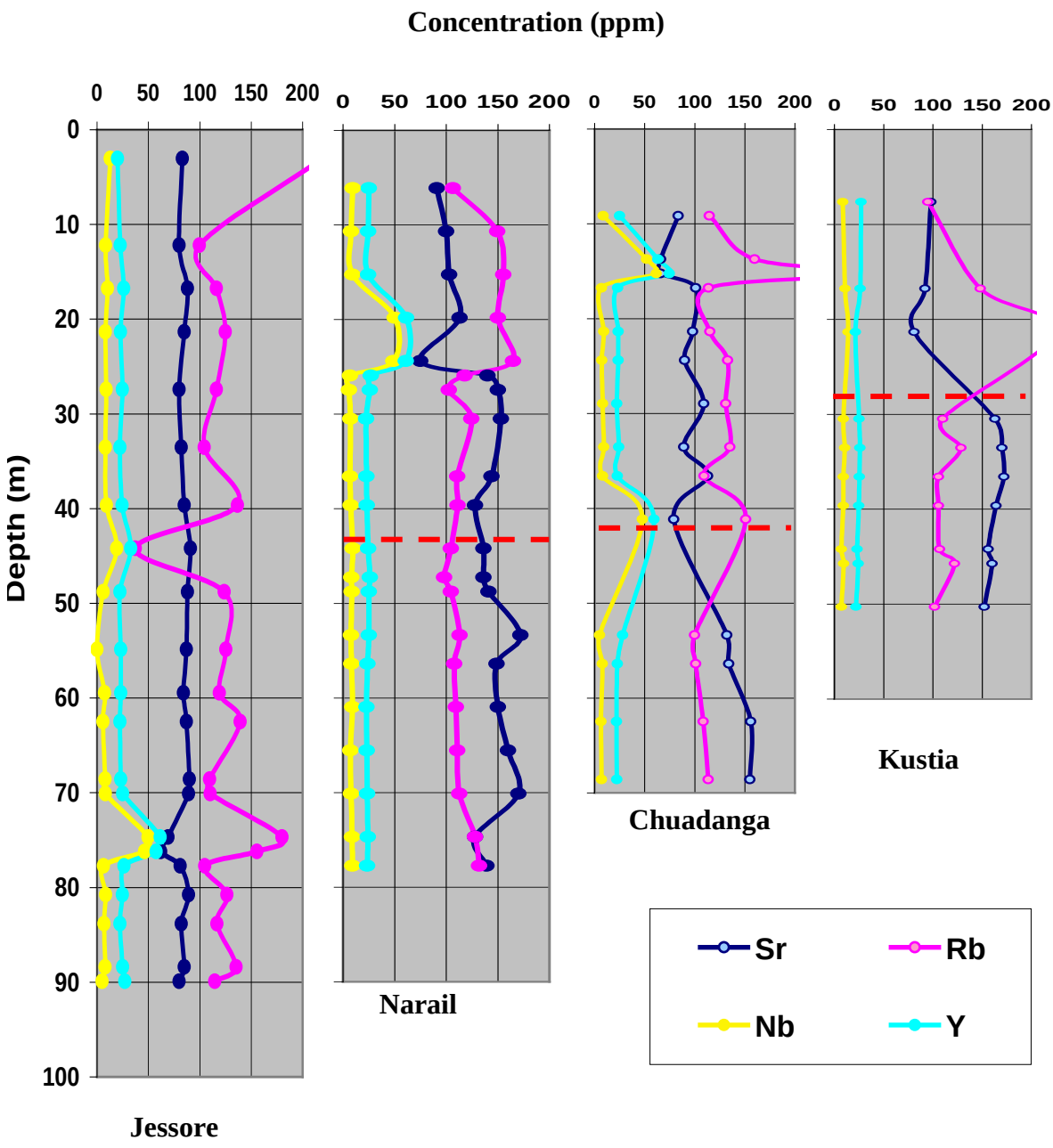

Figure 3.9: Down borehole concentrations of Sr, Rb, Nb and Y from the four boreholes in the present research. The red dashed line on the figure represents the Holocene-Pleistocene boundary.

3.7 Sr Geochemistry

There are two ways in which to treat the discussion of a trace element. One method involves the distribution of the trace element in various geologic systems, with no particular regard to any other element. A second method is to relate the trace element to a major element with which it has natural associations. There is the tendency for certain trace elements to follow major elements that are similar to them in ionic radius and charge (Goldschmidt, 1964). This latter method has proven useful for strontium when compared to calcium (Turekian and Kulp, 1956).

On the most general level, there are certain trace elements that substitute for one or more major rock forming elements in preference to others. Strontium has the same number of positive charge as calcium with slightly larger ionic radius. Therefore, Sr is a common element in the calcium-rich minerals and to an equal or lesser extent in high-temperature potassium minerals. To a first approximation, the mineral group responsible for both the calcium and strontium content of a silicate rock is the feldspar group. Certain pyroxenes and amphiboles may also be important in the distribution of strontium and calcium. However, they were not considered in the present study because of their low abundance in the borehole sediments.

There is an overall strong positive correlation between Sr and Ca concentration obtained from all available boreholes in the Bengal Basin (fig 3.10). An attempt was made to calculate the percentages of Ca-bearing feldspar minerals in the samples, and it was found that the minerals, which are actually controlling the Ca content of these borehole sediments, are Anorthite, Epidote and Apatite.

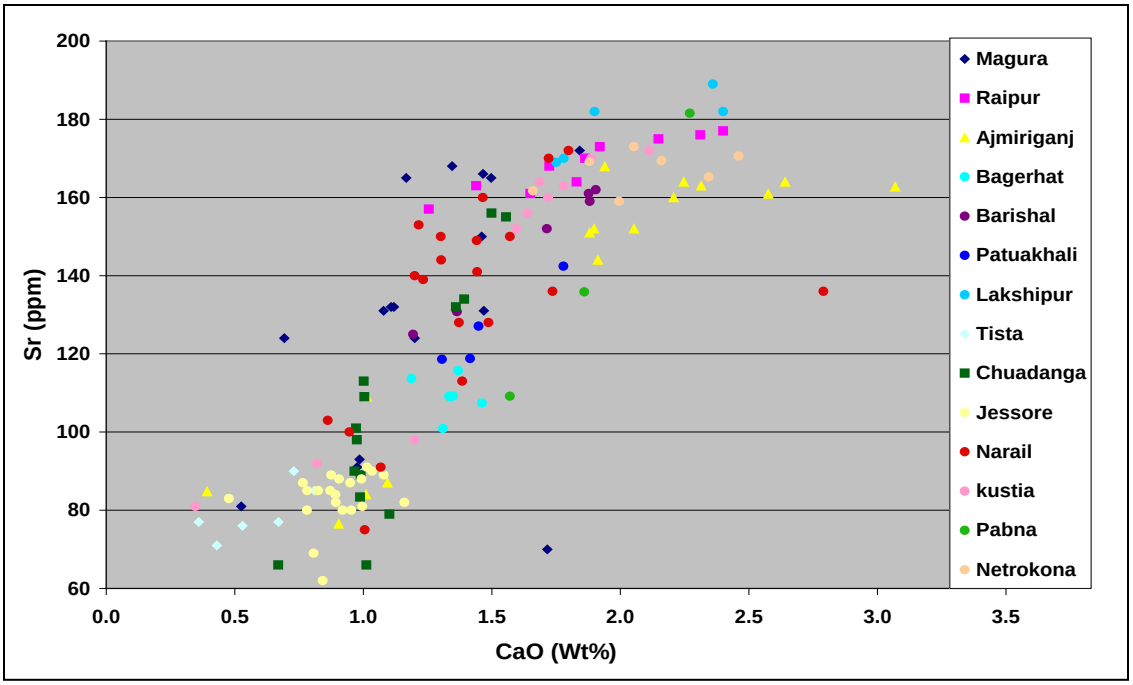

Figure 3.10: Plot of Sr versus Ca concentrations for all available Bengal Basin boreholes. Data show a distinct overall correlation between Sr and Ca concentration, probably related to source lithologies (Data from this study and Pate, 2008).

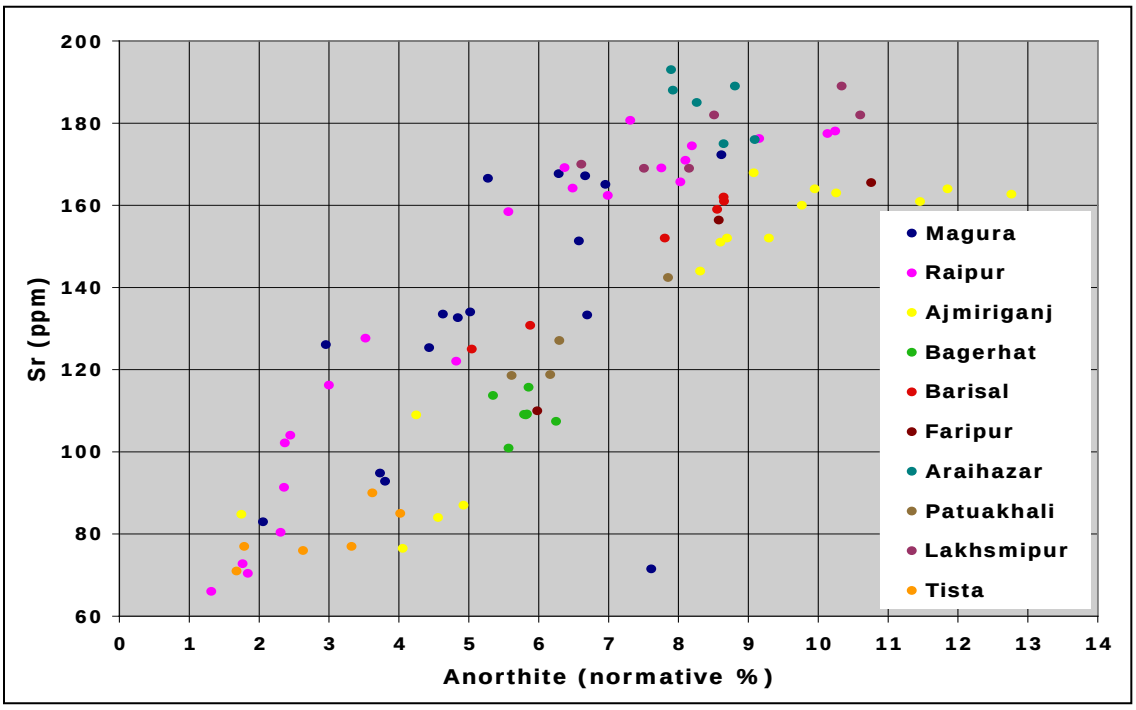

Figure 3.11: Plot of Sr versus anorthite content for all available Bengal Basin boreholes. Data show a distinct positive correlation between Sr and anorthite (Data from this study and Pate, 2008).

Weathering affect on Sr concentration

Sr can be mobile during weathering; hence, both original concentration and isotopic composition of sediments may be altered. However, Singh and Lanord, 2002 in their study on Himalayan erosion in the Brahmaputra watershed showed that a maximum of only 1.5% of the bulk sediment Sr might have been exchanged during weathering. Therefore, Sr signatures of sediment collected for this project can be considered as reflecting the primary Sr signatures of the source rocks. A plot of Otha Weathering Index (relative weathering indices based on major element concentration) versus Sr concentrations of all available borehole sediments from the G-B delta does not show any apparent correlation between these two. A wide range of Sr concentration from 60 to 180 ppm can have the same weathering index from 0.5 to 1.5. The relative weathering indices of the samples also reveal that the majority of the borehole sediments are not weathered.

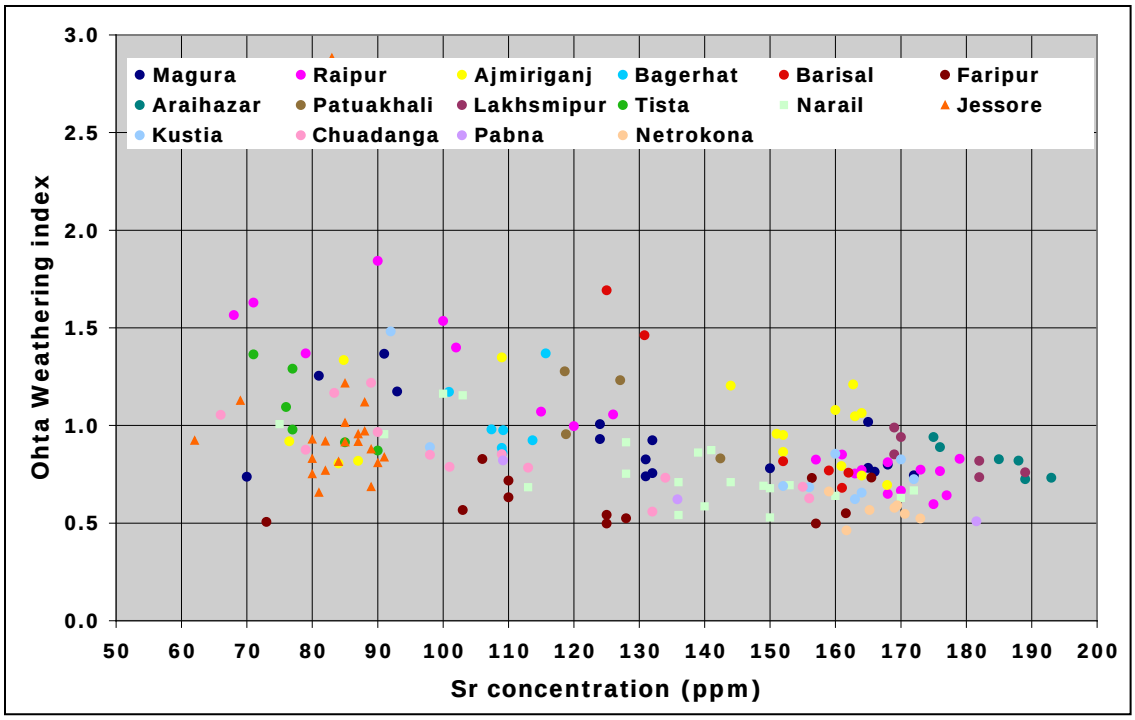

Figure 3.12: Plot of Sr versus Otha weathering index for G-B basin boreholes. Note the apparent lack of correlation between Sr concentration and Otha weathering index.

Grain size affect on Sr concentration

Figure 3.13 shows Al/Si versus Sr concentrations for all available Bengal Basin boreholes and Figure 3.14 shows grain size versus Sr concentrations for the studied four boreholes. There is an apparent lack of correlation between Sr concentrations and grain size within the sand grain-size fraction in both cases, which implies that Sr concentration is not dependent on grain size and thus can work as a robust provenance indicator for sand-sized sediment. The ratio of Al to Si is used here as a proxy for grain size because Si is the primary constituent in sand and Al is common within finer grained clays and feldspars. Figure 3.13 also demonstrates the higher Al_2O_3/SiO_2 ratio of southern and eastern boreholes, which are nearer to the coast where grain size is finer. Figure 3.14 shows two distinct populations of Sr concentration data. Along the upper group, the Sr concentration values ranges from 140- 170 ppm and fall within the Sr concentration range of the Brahmaputra derived sediments. The lower trend that has a Sr concentration range of 70-110 ppm, matches with the Sr concentration values of the Ganges derived sediment. Both of the trends of Sr concentrations is independent of grain size and has a constant gap in between them, which may suggest two different source areas for these two distinct trends.

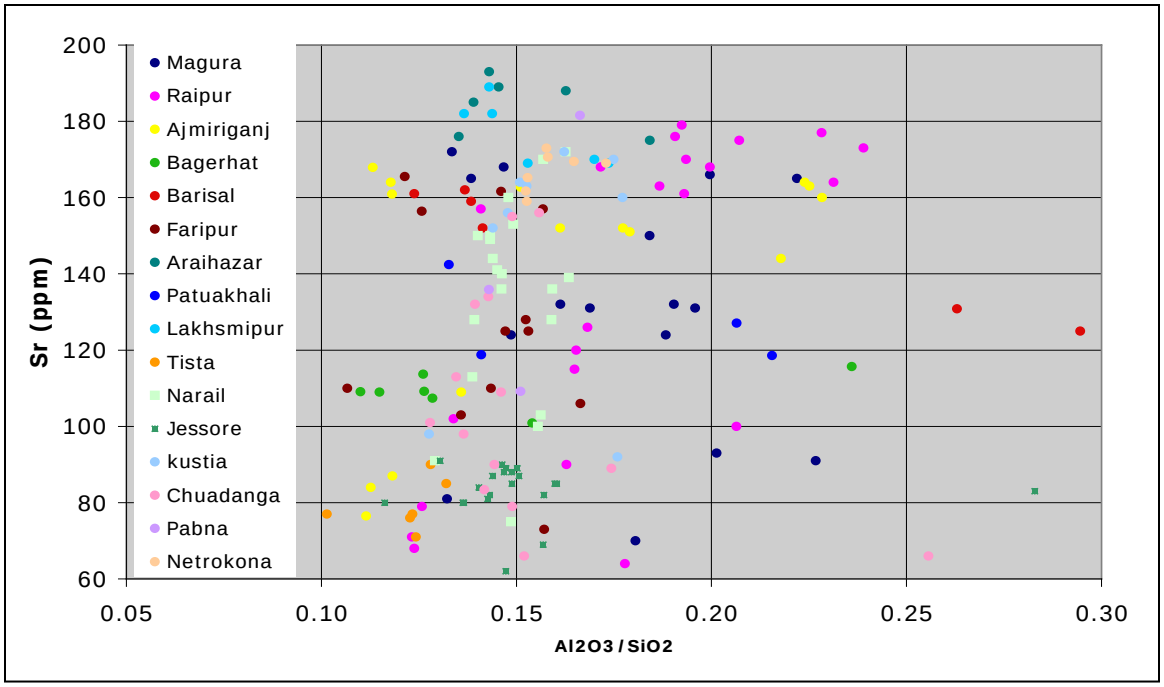

Figure 3.13: Al_2O_3/SiO_2 versus Sr concentrations for all available Bengal Basin borehole data (> 63 um) (data from this study and Pate, 2008).

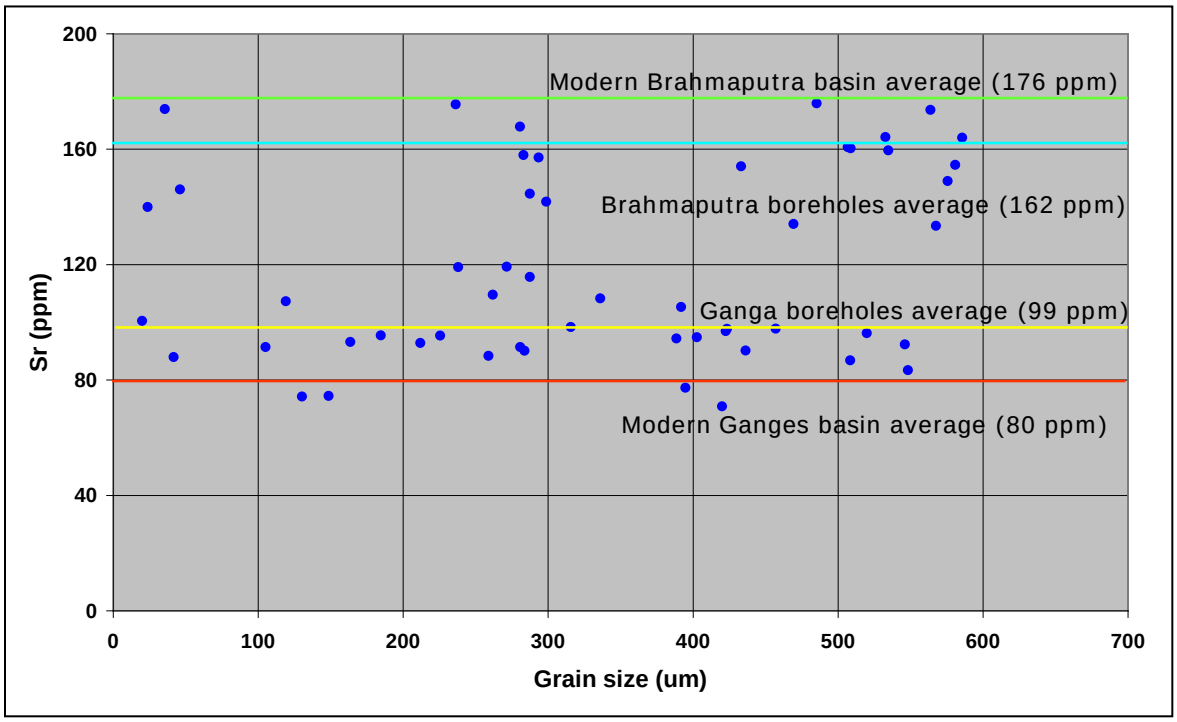

Figure 3.14: Grain size versus Sr concentrations for all available Bengal Basin borehole data (> 63 um) (data from this study and Pate, 2008).

3.7.1 Sr Concentrations of the borehole sediment

Except Jessore borehole, that has a 90-meter thick Holocene sequence, Sr concentration data from the other three boreholes show significant down-core trends for the Holocene and Pleistocene sediments (figure 3.19). The Pleistocene deposits usually have much higher Sr concentrations than the Holocene in Chuadanga, Kustia and Narail, which is manifested by the decreasing upward trend of Sr concentration. Jessore shows the lowest Sr concentration values throughout 90 meters of Holocene sequence. There is a sharp increase in Sr concentrations across the Holocene-Pleistocene boundary in Kustia and Chuadanga. However, Narail is the only exception where Holocene deposits also show higher Sr concentrations in the lower section.

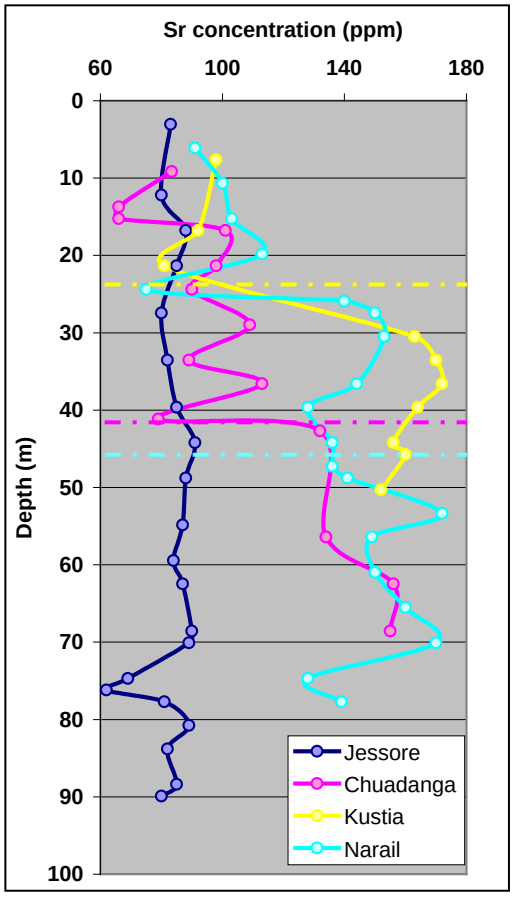

Figure 3.15: Down-hole Sr concentrations from the studied four boreholes. Dashed lines represent the Holocene – Pleistocene boundary in the respective boreholes.

Figure 3.16 shows a histogram of Sr concentration data from the studied four boreholes (a) and from all available studies within the Bengal Basin (b). Both of these histograms show a wide range of strontium concentration values ranging between 60 and 195 ppm. Taking account of the Sr concentrations of the various Himalayan domain, the Sr concentrations cluster within four major groupings defined as “Very low” from 60-70 ppm, “Low” from 70-100 ppm, “Intermediate” from 100 to 140 ppm, and “High” from 140- 195 ppm. Both the “Low” and “High” domain in the histograms shows normal distribution curves with distinct peaks at 90 and 170 ppm respectively. The intermediate values seem to be in a mixed zone enclosed by an extension of the normal distribution curves of the “Low” and “High” values.

One contrasting difference between these two histograms is that bulk of the samples from the studied four-borehole fall in the “Low” Sr group; while considering all boreholes throughout the Bengal basin, the major share of samples belongs to the “High” Sr concentration zone. The “Intermediate” group also shows higher proportions of samples for all Bengal Basin boreholes compared to the studied four boreholes. This may be because the four boreholes from this study were located in the south-west part of Bengal Basin signifying different sediment sources or fluvial inputs.

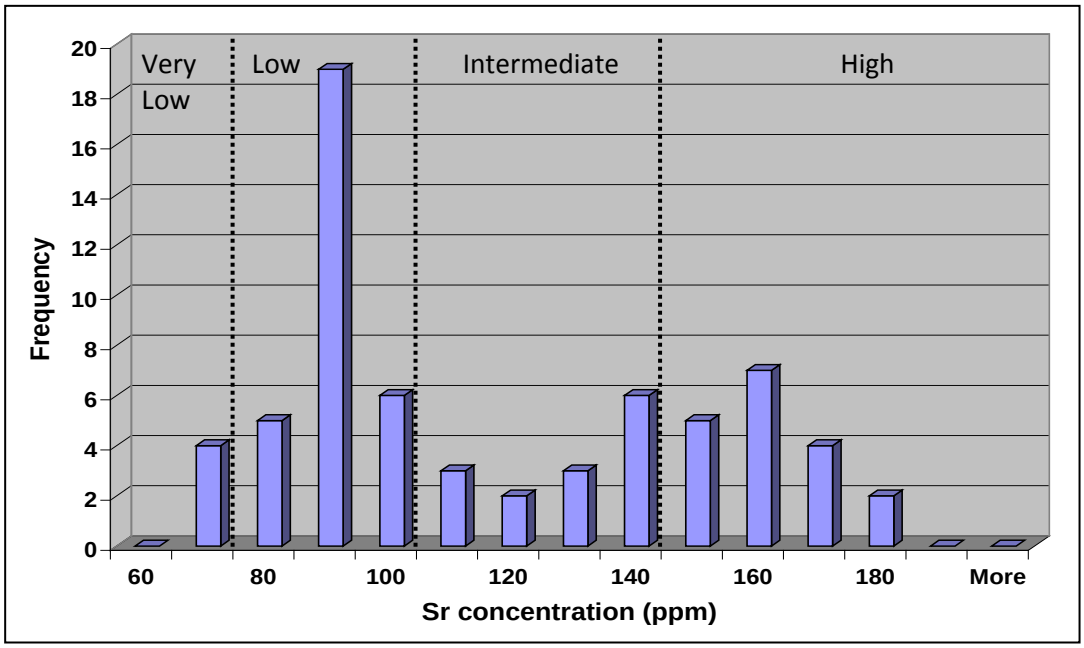

(a) Histogram for Sr concentration data from the studied four boreholes

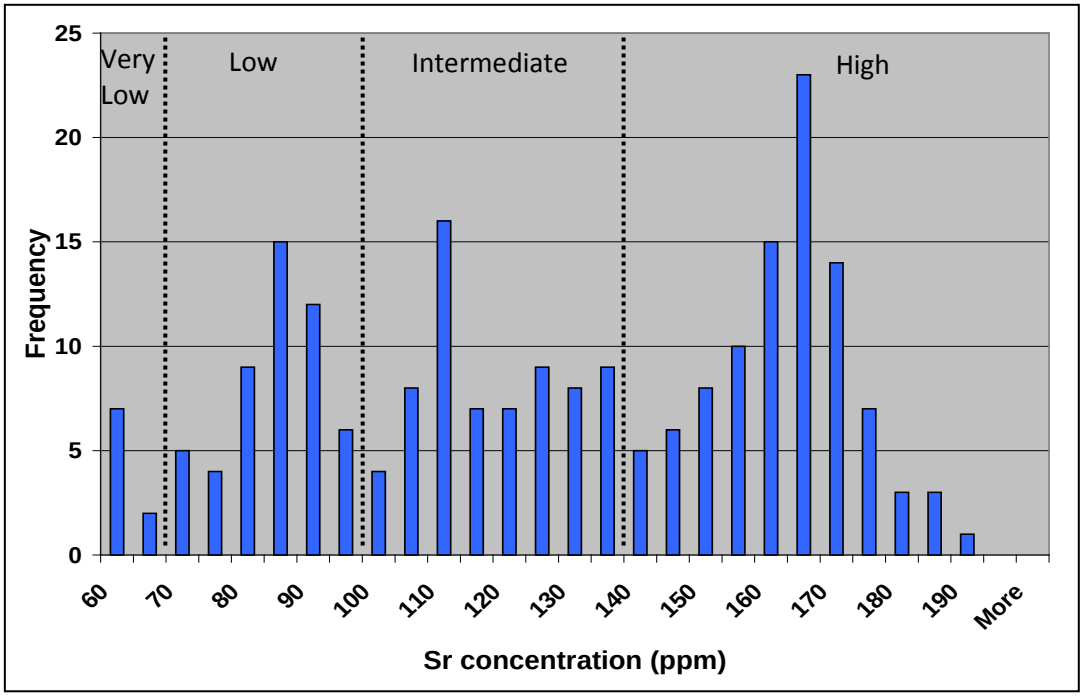

(b) Histogram for all available Bengal Basin Sr concentration data.

Figure 3.16: Histogram of Sr concentrations measured from the studied four boreholes and all available boreholes in the Bengal Basin. Data are grouped into “Very low”, “Low”, “Intermediate”, and “High” Sr categories.

3.7.2 Sr Isotope ratios

Figure 3.17 shows the histogram of strontium isotopic ratios measured from nine borehole samples including three of the four boreholes in this study. The Sr isotopic values in these samples show a wide range of values from 0.725 to 0.81. By comparing these values with the isotopic values in their source areas in Himalaya and Tibet, they can be clustered into four groups – "Low", "Intermediate", "High" and "Very High". Unlike the Sr concentration histogram where most of the samples fall in the "High" group, majority of the isotopic ratios in figure 3.17 fall in the "Low" group. Figure 3.18, which is a plot of Sr concentrations verses the isotopic ratios of the studied four borehole samples, also shows this reverse correlation between Sr concentration of the sediment and its isotopic ratios.

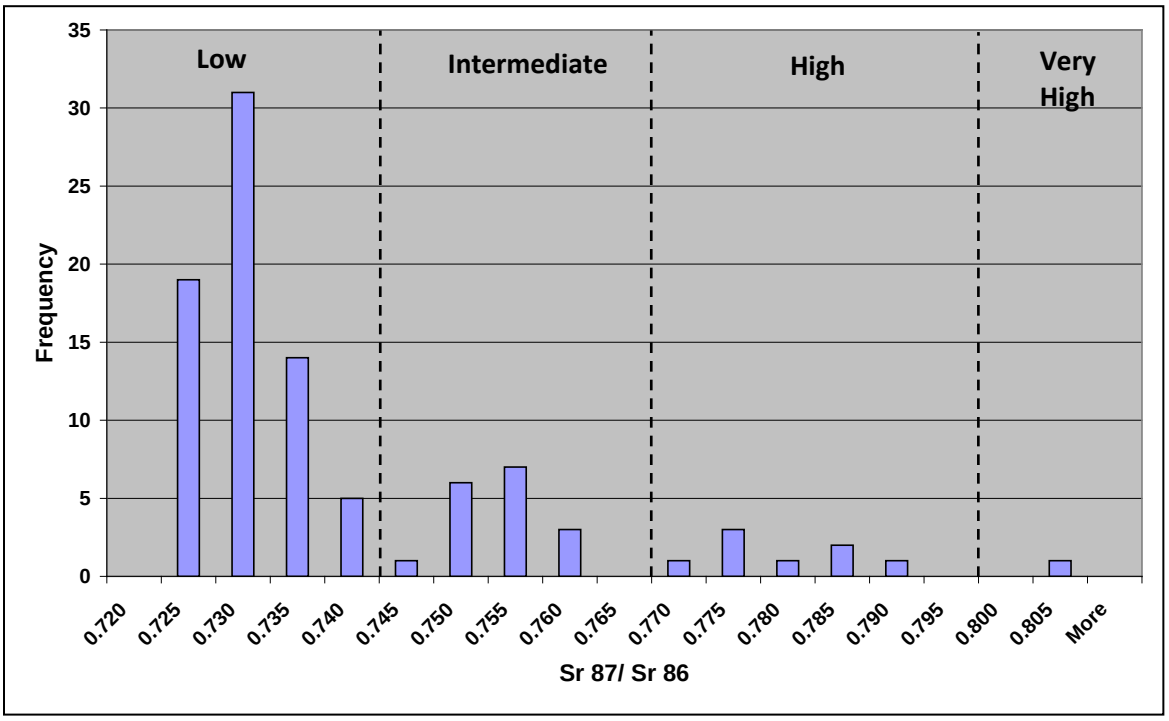

Figure 3.17: Histogram of Sr isotopic ratios measured from nine boreholes including the ones in the present study. Data are grouped into "Low", "Intermediate", "High" and "Very High" categories.

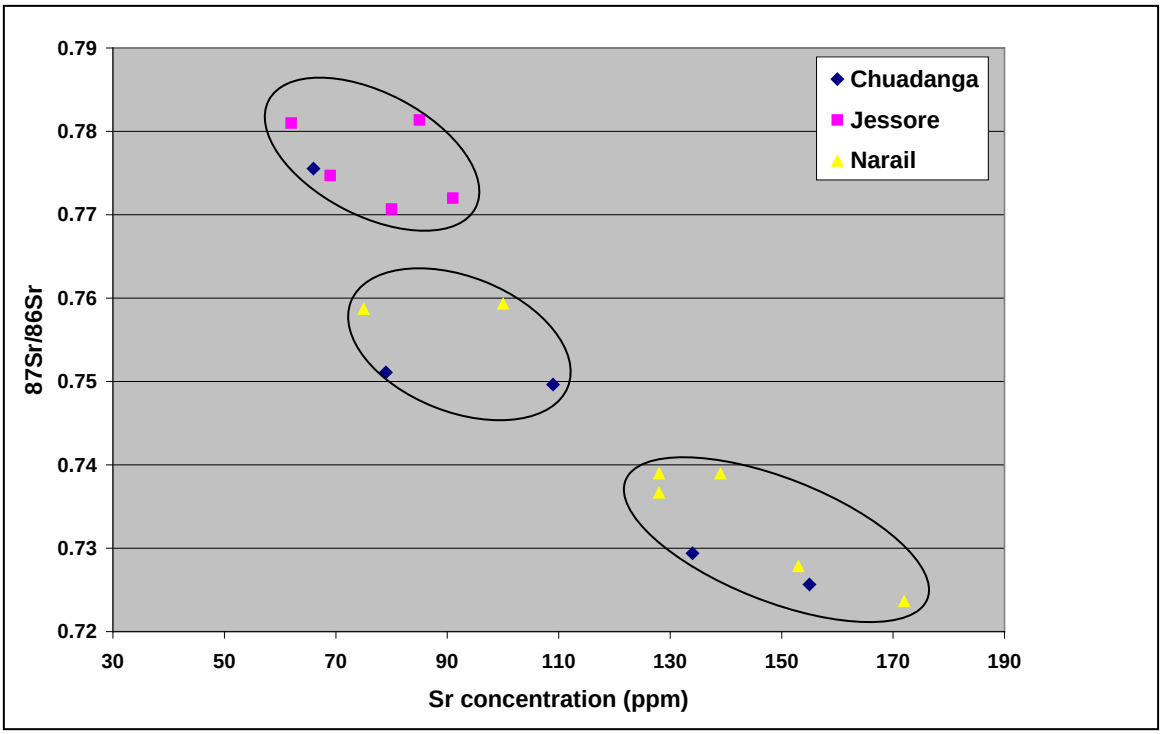

Figure 3.18: Plot of Sr concentrations versus isotopic ratios of the borehole samples in the present study showing three distinct sets of values.

The plot of Sr concentration verses isotopic ratios of the samples in the present study shows three distinct domain- "High" Sr concentrations with "Low" isotopic ratios, "Intermediate-Low" Sr concentrations with "Intermediate" isotopic ratios and "Low- Very Low" Sr concentrations with "High" isotopic ratios.

CHAPTER IV

Discussion

4.1 Sediment Provenance

The provenance analysis in this study is pursued using the total strontium concentration, $^{86}Sr/^{87}Sr$ ratios and the Nd isotopic ratios of the sediments collected at different depths from the boreholes in the present and previous studies in various parts of the G-B delta.

4.1.1 Total Sr concentration

Although the traditional approach for provenance studies in the Himalayan region involves only Sr isotopic ratio, Sr concentration can also be a useful new method. The biggest advantage of using Sr as a provenance indicator is its ability to preserve the geochemical fingerprints from distinct catchment lithologies. Moreover, it is easier and less expensive to generate Sr concentration data using XRF.

A histogram of all Sr concentration data measured from Bengal Basin sediment was discussed in the previous chapter where it has shown that the Sr concentrations of the borehole sediments deposited in the Late Quaternary can be grouped into “Very Low”, “Low”, “Intermediate” or “High”. Figure 4.1 represents the same histogram but in this case, different color codes have been used to relate those Sr concentration groups with their respective provenances. It shows that the Late Quaternary deposit in the G-B delta had derived from all the major source areas in the Himalayas and Tibet.

The sediment in the G-B delta that has “High” Sr concentrations more than 140 ppm was most likely transported by the Brahmaputra River, because only the Brahmaputra drains the Tethyan Himalayan Sedimentary Sequence and the young batholiths from the Tibetan area (Singh and Lanord, 2002; also see figure 1.4). However, these two source areas did not contribute the

biggest fraction of Brahmaputra sediment deposited in the G-B delta during the Late Quaternary. This is obvious from the fact that the Sr concentrations of the rocks of Tibetan Plateau and Tethyan Himalaya, which are 400 ppm and 200 ppm respectively, are much higher than the average Sr concentration (173 ppm) of the Brahmaputra borehole sediment found in this study. Therefore, it is more likely that nearly 50% of the Late Quaternary Brahmaputra sediment were derived from the Higher Himalayan province in the Namche Barwa–Gyala Peri massif in the Eastern Syntaxes, that caused this drop in Sr concentration from as high as 400 ppm to as 1ow as 173 ppm. Published mineralogical and geochemical data also suggest that the eastern syntaxis contributes fully 50% of the total sediment flux of the Brahmaputra and ~20% of the total detritus reaching the Bay of Bengal (Singh and France-Lanord, 2002; Garzanti et al., 2004; Tibari et al., 2005). Stewart et al. (2008) in their research on Namche Barwa–Gyala Peri massif, provided a more precise estimate of Brahmaputra sediments coming out from this source region. From the simple mixing models of U-Pb ages on detrital zircons from samples taken above and below the massif, they found an average exhumation rates of a 7–21 mm yr^{-1} in an area of ~3300 km^2 centered on the massif. Stewart et al. (2008) suggest that this rapid exhumation, which is consistent with the very young cooling ages (0.6 Ma) of the detrital zircons from this area, produces so much sediment that ~50% of the Brahmaputra load at the front of the Himalaya comes from only ~2% of its drainage.

The Late Quaternary sediment in the G-B delta that has “Low” Sr concentrations between 70 and 100 ppm (fig. 4.1) most likely derived from the Ganges River because ~80% of Ganges sediment are coming from the Higher Himalaya (Wasson, 2003), which has a low Sr concentration. Moreover, the Ganges has < 10% sediment input from the Tethyan Himalayan Sequence and the Tibetan Plateau (Wasson, 2003). Instead, ~ 20% of Ganges sediment is coming from the lesser Himalaya and from the Himalayan Fore deep with Sr concentrations < 70 ppm, which is even lower than the Higher Himalayan rock (Singh, 2008).

"Very Low" (<70 ppm) Sr concentrations on the histogram is interpreted to be sediment deposited directly by the Tista river. Tista is the only Himalayan River, which might have had a direct input of Lesser Himalayan sediment into the G-B delta during the Late Quaternary. The "Intermediate" (110-140 ppm) Sr concentrations on the histogram most probably represent a mixing between Ganges and Brahmaputra sediment. Although, it was not possible in the present study to determine the relative proportions of the Ganges vs. Brahmaputra input because the Ganges and Brahmaputra input themselves comprise variable mixtures.

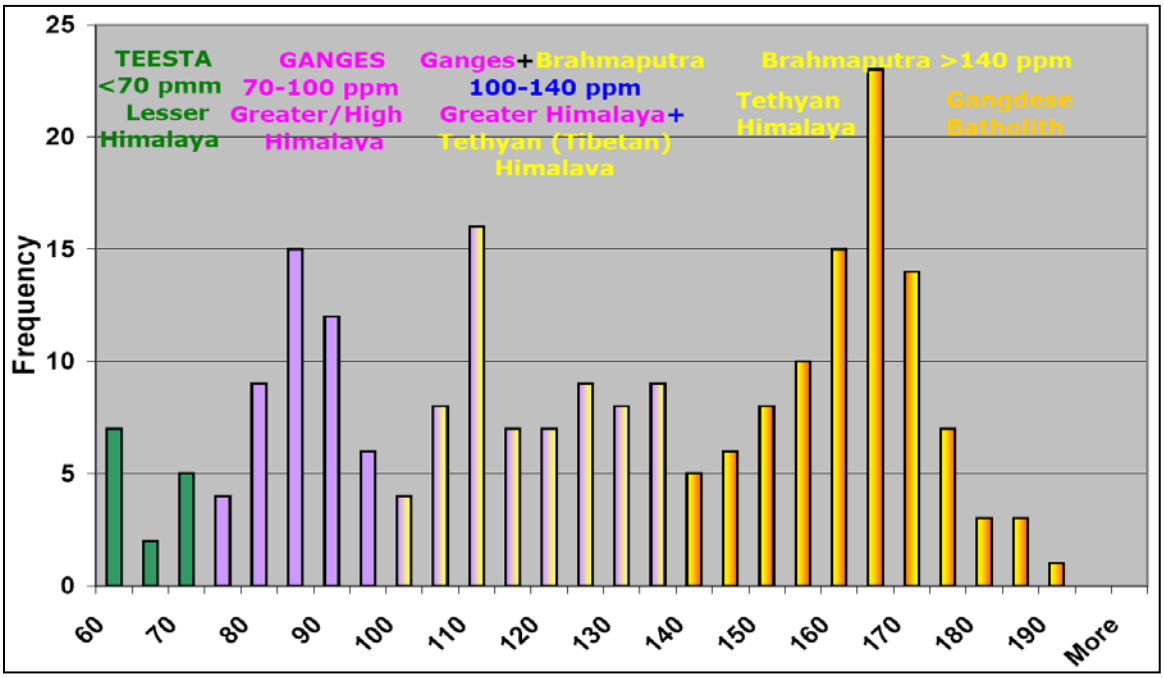

Figure 4.1: Histogram for Sr concentration data from all available borehole sediment including those used in the present study.

Figure 4.1 shows that most of the Late Quaternary sediments in the G-B delta were deposited by Brahmaputra River. It also implies that a large portion of the Late Quaternary G-B delta sediment have their provenances in the Tibetan Plateau and in the Tethyan Himalaya. However, the Higher Himalaya, which is a common sediment source of both the Ganges and Brahmaputra rivers, seems to supply the bulk of the sediment during both the Holocene and Pleistocene. Figure 4.2 and figure 4.3 shows that almost all of the Brahmaputra sediment found in

the present study area are actually deposited during the Late Pleistocene. Figure 4.2 (a), which is histogram of Sr concentrations of the Holocene samples shows the presence of few Brahmaputra sediments in the Holocene period. However, figure 4.2 (b) does not show a single Pleistocene sample that has Sr concentration less than 100 ppm. Therefore, it can be presumed that during the Late Pleistocene, primarily the Brahmaputra built the delta from Chuadanga eastward. It can be also assumed that Ganges River had less influence on the sedimentation in the G-B delta during this time. However, the patterns of sediment dispersal in the G-B delta have changed from the Early Holocene, when the Ganges river system started to contribute a large portion of sediment to the delta stratigraphy. The domination of Ganges sediment over the Brahmaputra in the western delta since the Early Holocene is also manifested by the figure 4.2 (a) and 4.3. It is clear from the data that the major portion of the sediment has a Sr concentration range from 70-100 ppm, which is same as the Sr concentrations of the Ganges suspended sediment derived from Higher and Lesser Himalaya. A comparatively smaller proportion of pure Brahmaputra (>140 ppm) and "mixed" (100-140 ppm) Holocene samples also indicate the waring influence of the Brahmaputra in the western delta starting from Early Holocene.

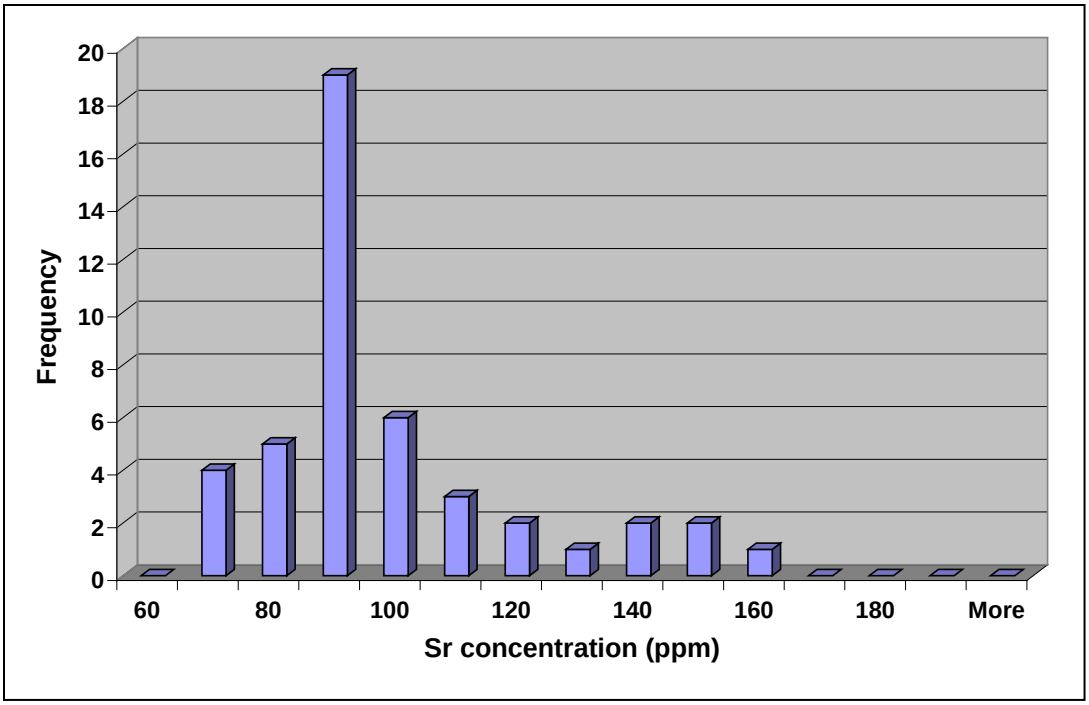

Figure 4.2 (a): Histogram for Sr concentrations of the Holocene samples from the studied four boreholes showing the domination of Ganges input over the Brahmaputra.

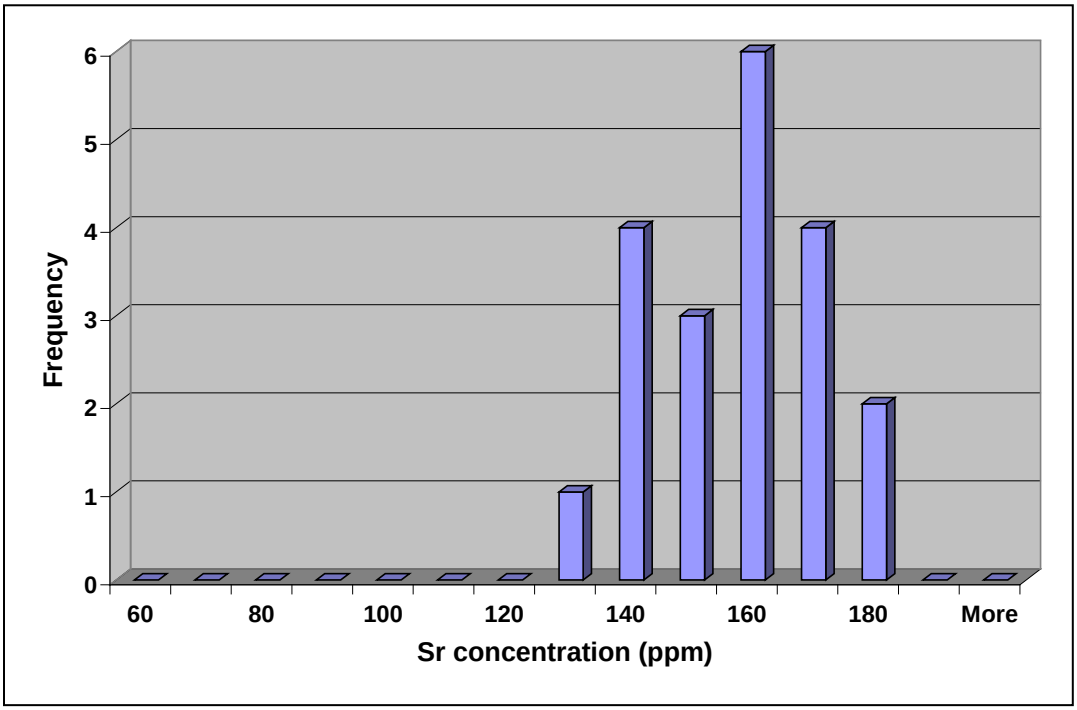

Figure 4.2 (b): Histogram for Sr concentrations of the Pleistocene samples from the studied four boreholes showing very little Ganges input.

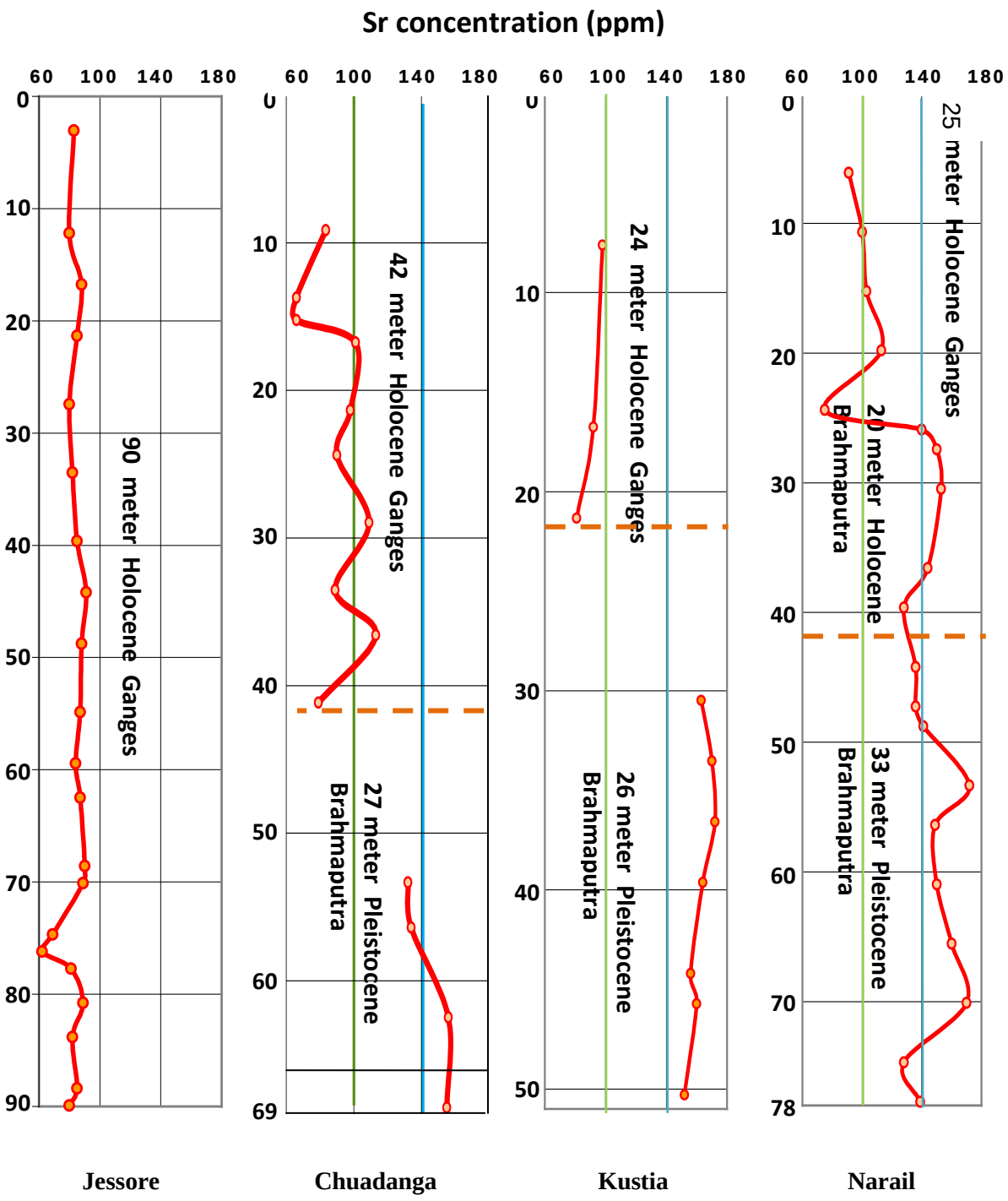

Figure 4.3: Down borehole Sr concentrations from the studied four boreholes showing the presence of only Brahmaputra sediment in the Pleistocene and the domination of Ganges sediment in the Holocene. Green and blue lines distinguish Sr provenance groups outlined in figure 3.16; dashed orange lines represent the Holocene – Pleistocene boundary.

4.1.2 Sr isotopic ratios

Figure 4.4 shows a plot of Sr concentration versus the Sr isotopic ratios for the sediments transported by the Ganges, Brahmaputra and by the other Himalayan Rivers in their various upstream areas. The figure shows a wide range of values both for Sr concentrations (30 ppm – 250 ppm) and isotopic ratios (0.71 – 0.84) indicating distinct source areas for these rivers. Defining these end member sources as well as their concentrations and isotopic ratios is a prerequisite for the provenance analysis of the G-B delta sediment. Therefore, before making any provenance analysis based on isotopic ratios, we would like to find out the average isotopic values of the sediments transported by various Himalayan, Tibetan and Shillong rivers so that we can compare the Sr concentrations and the isotopic values from our boreholes with this end member values to confirm their Himalayan or Tibetan sources.

Figure 4.4 shows that Brahmaputra river sediment (blue circles) have a wide range of Sr concentrations from 150 ppm to as high as 250 ppm but their isotopic ratios show a relatively narrow range between 0.715 to 0.73. The average Sr concentration of the sediment of the Brahmaputra end member is therefore as high as 176 ppm with a relatively low isotopic ratio of 0.725 (blue square). It is quite interesting to note that the sediments eroded from the Shillong plateau (yellow circles) have the same range of isotopic ratio between 0.72 and 0.73. However, the Shillong sediments are distinguishable from the Brahmaputra or Tibetan sediments by their very low Sr concentrations. The average Sr concentration and the isotopic ratio of the Shillong end member sediment is 72 ppm and 0.735 respectively.

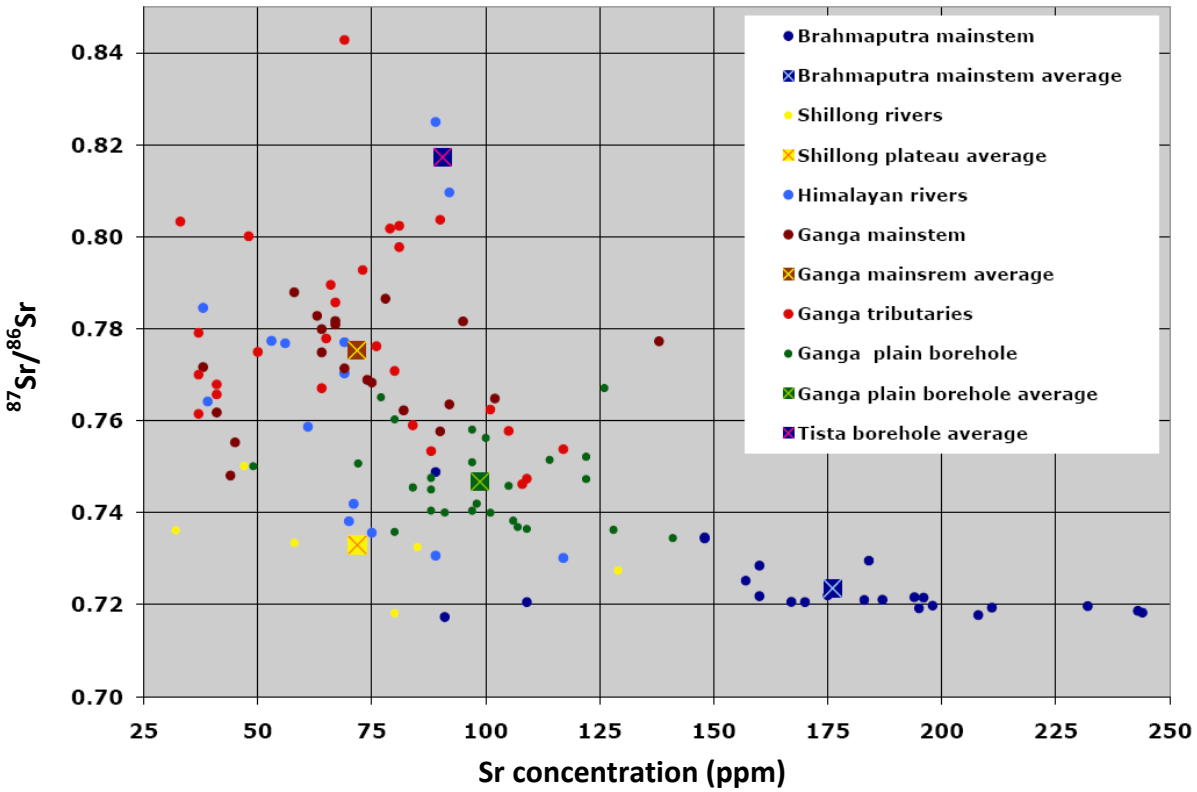

Figure 4.4: $^{87}Sr/^{86}Sr$ values plotted against Sr concentration for Tibetan samples (i.e., Brahmaputra) and Himalayan samples (i.e., Ganges). Data are from direct sampling of Brahmaputra, Ganges, Tista and other Himalayan riverbank and suspended sediments as well as borehole sediments (compiled from Derry and France-Lanord,1997; Galy et al.,1999; Singh and Lanord, 2002; Singh et al., 2006).

The third end member source for G-B delta sediment is the Higher Himalaya, which is represented by the sediments transported by both Ganges mainstem (brown circles) and its northern tributaries (red circles). Like the Brahmaputra River, the Ganges mainstem sediment also show a wide range of Sr concentrations, though the concentration values are far less compared to the Brahmaputra sediment. The Sr concentration of the Ganges mainstem sediment ranges from ~ 50 to 100 ppm with an average of 72 ppm, which is same as the Shillong sediment. However, in contrast of the Brahmaputra (Tibetan) or the Shillong sediment, the Ganges sediment have a much higher average isotopic ratio of 0.775 with a range varying from 0.75 to 0.79. It is also interesting to compare the isotopic ratio values between the Ganges tributaries and the other

Himalayan Rivers (blue circles). The Ganges tributaries have a sediment mixture coming from the Higher and Lesser Himalaya whereas sediment transported by the other Himalayan Rivers considered in this study have a dominant Higher Himalayan source, which makes their isotopic ratio slightly lower than the sediments transported by the Ganges tributaries.

The fourth end member acting as a minor source for the G-B delta is the Lesser Himalayan Sequence, which is represented in this study by the sediments collected from the Tista borehole. As mentioned before, this end member shows the highest Sr isotopic ratio with a low to very low Sr concentration.

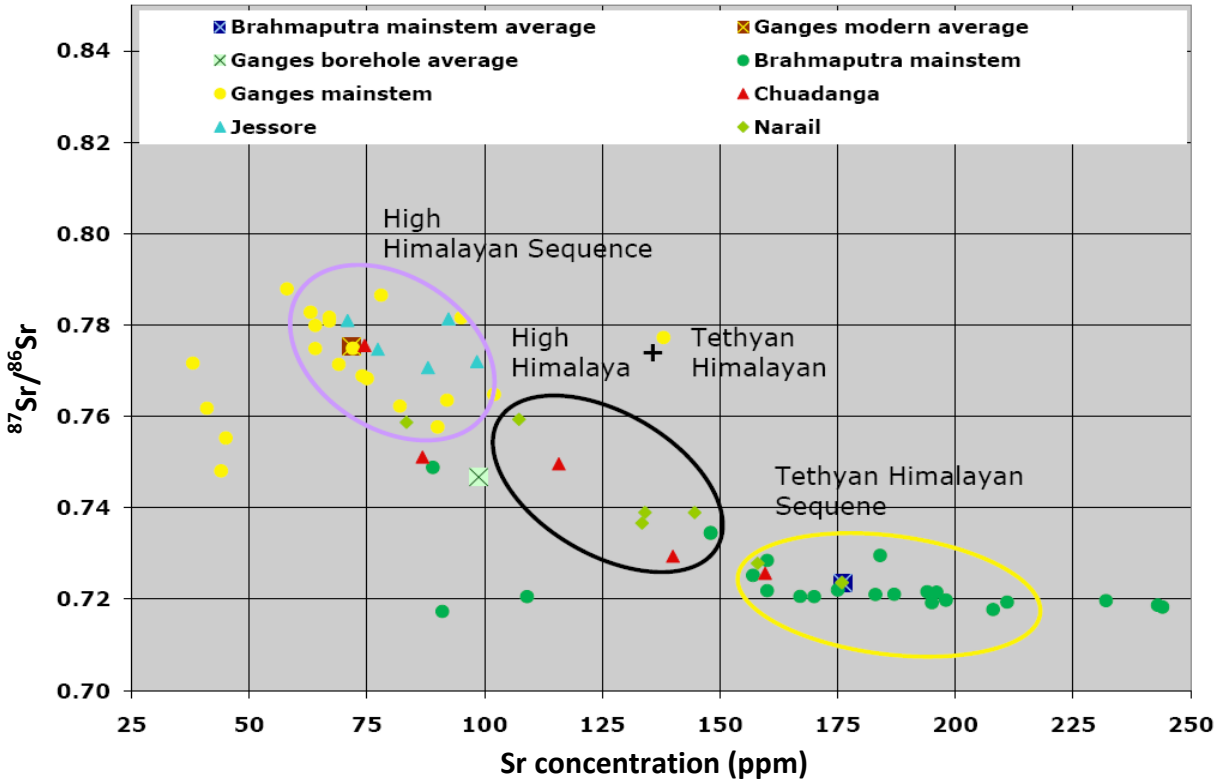

Figure 4.5: Plot of Sr concentrations versus the isotopic ratios for the samples collected for this research. The figure clearly shows that all of the studied samples fall within the High Himalayan or the Tethyan Himalayan domain or in between two.

An attempt of provenance analysis by comparing both the Sr concentrations and the isotopic ratios of the borehole samples with their various end members is made using the figure

4.5. From the figure, it is evident that the Holocene samples collected from the Jessore borehole have a dominant High Himalayan source given that all results plot within the Higher Himalayan domain. This supports our earlier interpretation that the major portions of the Holocene sediment deposited in the western delta were brought by the Ganges River.

Unlike the Jessore borehole, the samples collected from the Chuadanga and Narail boreholes show both the High Himalayan and Tethyan Himalayan signature. Among the five Chuadanga samples, only one falls within the Tethyan Himalayan domain that came from the Pleistocene deposit. Three other Chuadanga samples plot between the Tethyan and Higher Himalayan domain, suggesting that they are a mixture of Tibetan plateau and Higher Himalaya sources. The remaining Chuadanga sample has almost the identical Sr concentration and isotopic ratio of the sediment transported by the Modern Ganges River indicating its Himalayan origin. The Narail samples show the same trend of Sr concentration and isotopic ratio as those from Chuadanga. It is quite remarkable that in both Chuadanga and Narail, the isotopic ratios of the samples trend higher up through the stratigraphic sequence (see figure 4.10). This strongly suggests a gradual shifting of sediment provenance in the western delta from Tibetan to Himalayan starting from the early Holocene. The Chuadanga and Narail samples, which fall between Higher and Tethyan Himalayan domains, may represent a period between the Late Pleistocene and Early Holocene when there was an equal share of sediment from both Himalaya and Tibet.

As the data suggest that a major portion of the G-B borehole sediment are a mixture of at least two end members, an attempt was made using figure 4.6 to assess the input ratios from these different sources. Indeed, most of the borehole samples fall along one of the four mixing curves drawn between these end members. The position of the samples along these mixing curves also gives us a broad idea about the possible river courses that have built the G-B delta during Holocene.

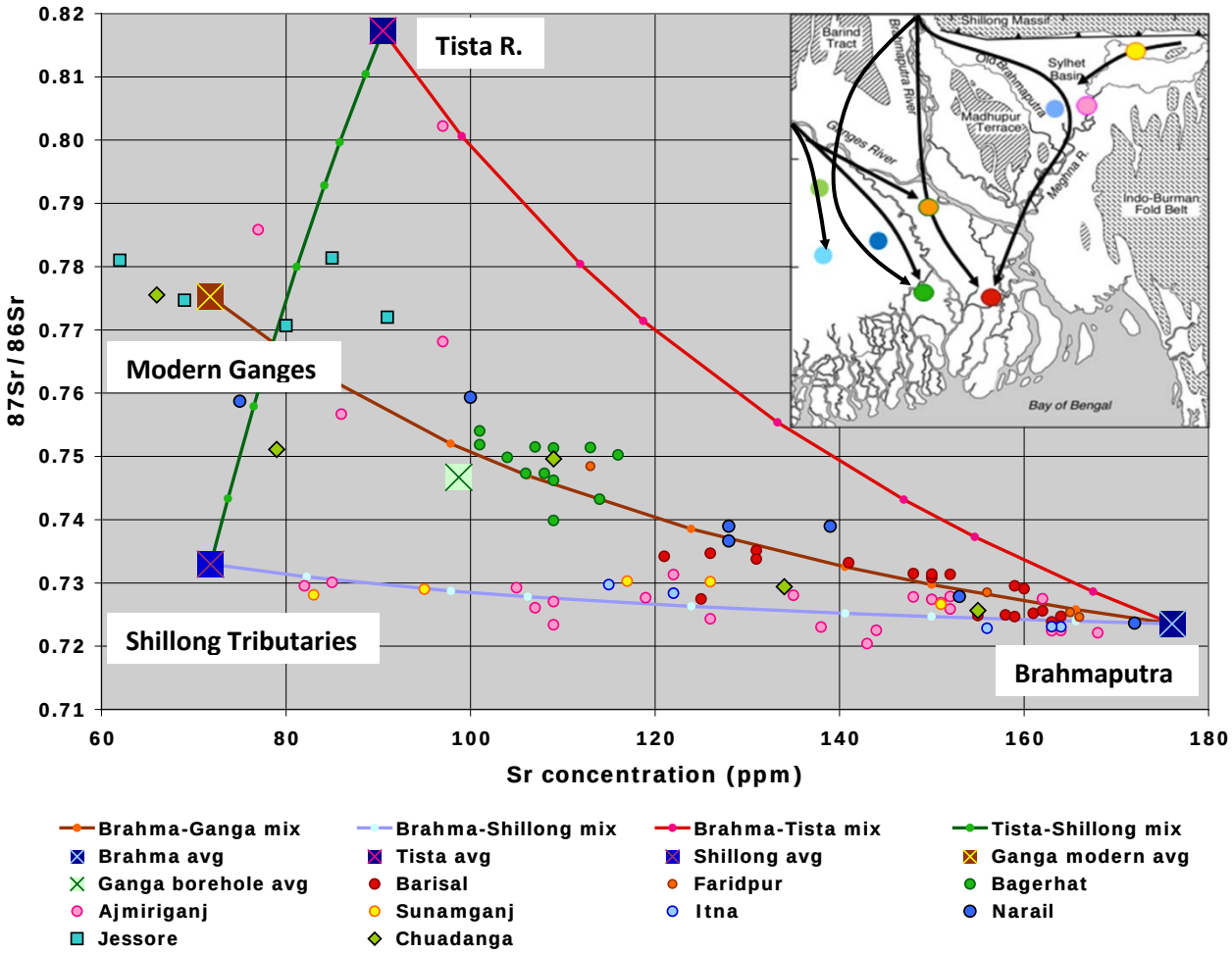

Figure 4.6: Showing the mixing curves that connect the end members representing the four major source areas for the G-B delta sediment. The inset map shows the location of the nine boreholes that are plotted on the mixing curve. The black arrow paths in the inset map also show the possible sediment transport route within the G-B delta during the Holocene. Data from this study, Youngs (unpublished) and Pate, 2008.

One prominent pattern discernable from figure 4.6 is that all northeastern borehole (Ajmiriganj, Sunamganj and Itna) samples plot along a mixing curve between Shillong tributaries and Brahmaputra member indicating their sediments are likely derived from both source terrains. Among these sites, Ajmiriganj and the Sunamganj include samples that may be as much as 90% derived from the Shillong massif. On the other hand, Itna, which lies along the old Brahmaputra River course, is primarily composed of sediments derived from the Brahmaputra.

Except for these three boreholes, all other available borehole samples plot along the mixing curve between the Brahmaputra and modern Ganges end members. It is also evident from the borehole location map that the eastern G-B delta borehole samples are closer to the Tibetan-influenced Brahmaputra end member and the western G-B delta borehole samples are closer to the High Himalayan influenced Ganges end member. For instance, the Barisal borehole data from the left edge of the eastern G-B delta plot close to the Brahmaputra end member on the mixing curve with some signature from the High Himalayan sediments. On the other hand, the Jessore samples collected from the western G-B delta are more inclined to the Higher Himalayan end member and more likely to be transported by the Ganges River. Most interestingly, Bagerhat borehole, which is located in the central delta between Barisal and Jessore, suggests a mixed source, with significant input from both Himalayan and Tibetan reaches.

4.1.3 Nd isotopic ratios

Figure 4.7 (a) shows the well-established εNd versus $^{87}Sr/^{86}Sr$ isotopic ratio plot for Higher Himalayan, Lesser Himalayan and Tibetan sediment proposed by Derry and France-Lanord (1997). Similar to the Sr concentration and isotopic ratios, εNd values of the rocks of various Himalayan and Tibetan domain are quite different from one another and provide a useful provenance indicator. After their detailed analysis on Himalayan and Tibetan rocks, Derry and France-Lanord (1997) proposed a specific range of Sr isotope and εNd values for various Himalayan and Tibetan domain.

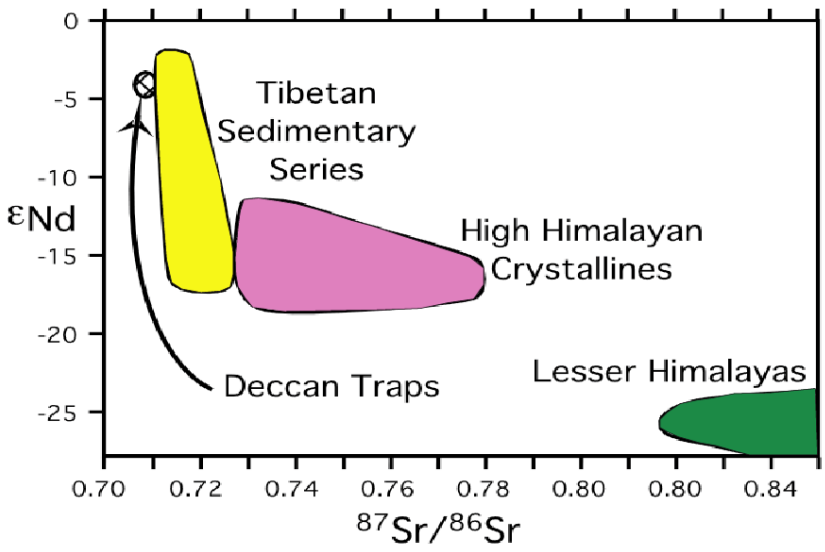

(a)

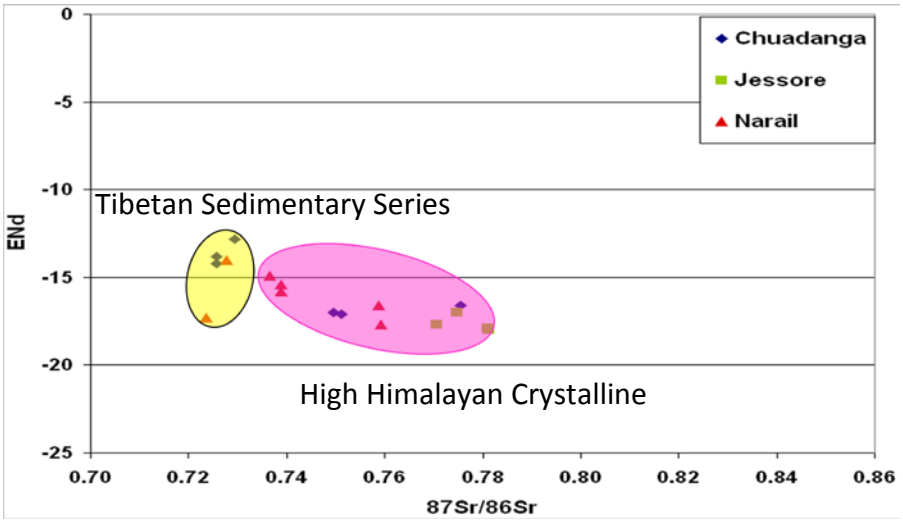

(b)

Figure 4.7: Plot of εNd versus $^{87}Sr/^{86}Sr$ isotopic ratio showing- (a) the already established εNd and Sr isotopic ranges for Higher Himalayan, Lesser Himalayan and Tibetan sediment (Derry and France-Lanord, 1997) and (b) two major group of sediments based on the measured εNd and Sr isotopic ratios for the present study.

Samples from only three boreholes from the present study were tested for their εNd values. The εNd values of these samples showed a relatively narrow range from -17 to -12

compared to the εNd values measured by Derry and France-Lanord. None of the 16 samples measured from the three boreholes shows εNd values smaller than -17. According to the Sr vs. εNd plot proposed by Derry and France-Lanord, none of these borehole samples falls within the Lesser Himalayan domain that has a minimum εNd value of -22. After comparing the figures in 4.7, it is also obvious that most of these G-B borehole sediments derived from either the Tibetan Plateau or the Higher Himalaya.

4.2 Late Quaternary Depositional System in the G-B delta

Based on the ranges of Sr concentrations in the individual boreholes, we propose three different depositional systems during the Holocene, which built most of the G-B delta controlled by the migration and avulsion of the Ganges and Brahmaputra River. The Holocene sequence in the far western delta is deposited almost exclusively by the Ganges River with a minor input from Tista. In this zone, no sample had a Sr concentration that exceeded 119 ppm (figure 4.8). Therefore, it is obvious that these western-most boreholes have no signature of Brahmaputra sedimentation. The most striking observation from this zone is that the Sr values are higher for the southern boreholes than the northern ones. One explanation is the southern part of this zone has some sediment that was eroded from the buried Pleistocene deposits of Brahmaputra origin.

Figure 4.8: Showing the Sr concentration ranges measured from the individual boreholes from all over the G-B delta. Borehole in yellow color represents only the Holocene sequence and the borehole in orange represents those boreholes, which has both Holocene and Pleistocene sequence. The values in yellow represent the Sr concentrations of the Holocene samples and the orange represent the Pleistocene ones.

We consider the central delta as the mixing zone between Ganges and Brahmaputra depositional system during mid-late Holocene. However, the early Holocene sediment do not show a mixed input, rather they are of Brahmaputra origin. There is a marked difference in Sr concentrations between the upper and lower Holocene in this zone. For example, in Faridpur the Sr concentrations drop to 113 ppm in the upper Holocene from 166 ppm in the lower Holocene. In Narail, the range drops from 133-158 ppm to 98-119 ppm. In Barisal, it decreases from 152-162 ppm to 125-131 ppm. Therefore, it is suggested that not only the Pleistocene but also the lower Holocene sediment in the central delta were deposited by Brahmaputra river system

starting from the Early Holocene. During the Mid to Late Holocene, the Ganges river avulsed from the west mingling with the Brahmaputra, which dropped the Sr concentrations in the upper Holocene.

In the Eastern G-B delta, the Holocene sequence was predominantly deposited by the Brahmaputra River eroding sediments from Higher Himalaya, Tethyan Himalaya and the Tibetan Plateau. However, there was also a second sediment transport route for this zone from the north-eastern Shillong plateau represented by its low Sr concentrations. Other than the three northeastern boreholes that had a direct sediment input from the Shillong, the Sr concentration values of the Holocene sequence in all other boreholes in the eastern delta range from 158-193 ppm without any signature of Tista input.

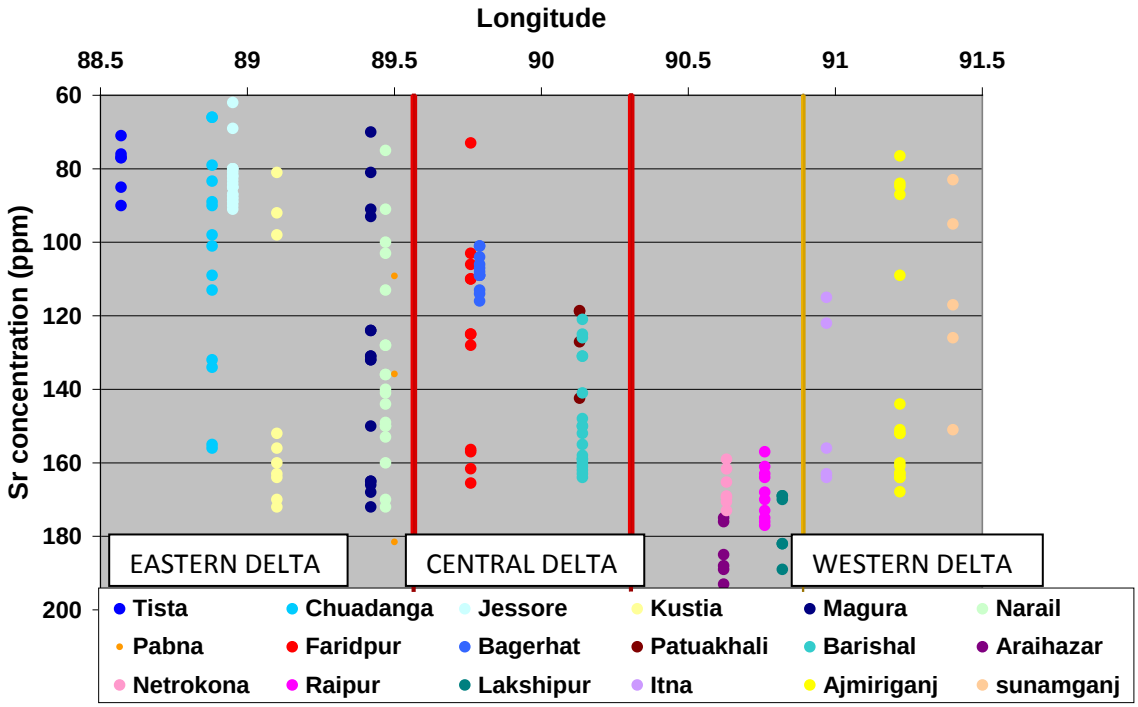

Figure 4.9: Showing the Sr concentration ranges for the Eastern, Central and Western delta. Note that except for the three western most boreholes, there is a gradual increase in Sr concentrations from the Eastern delta to the western delta indicating a basin ward migration of the river system from the west to east.

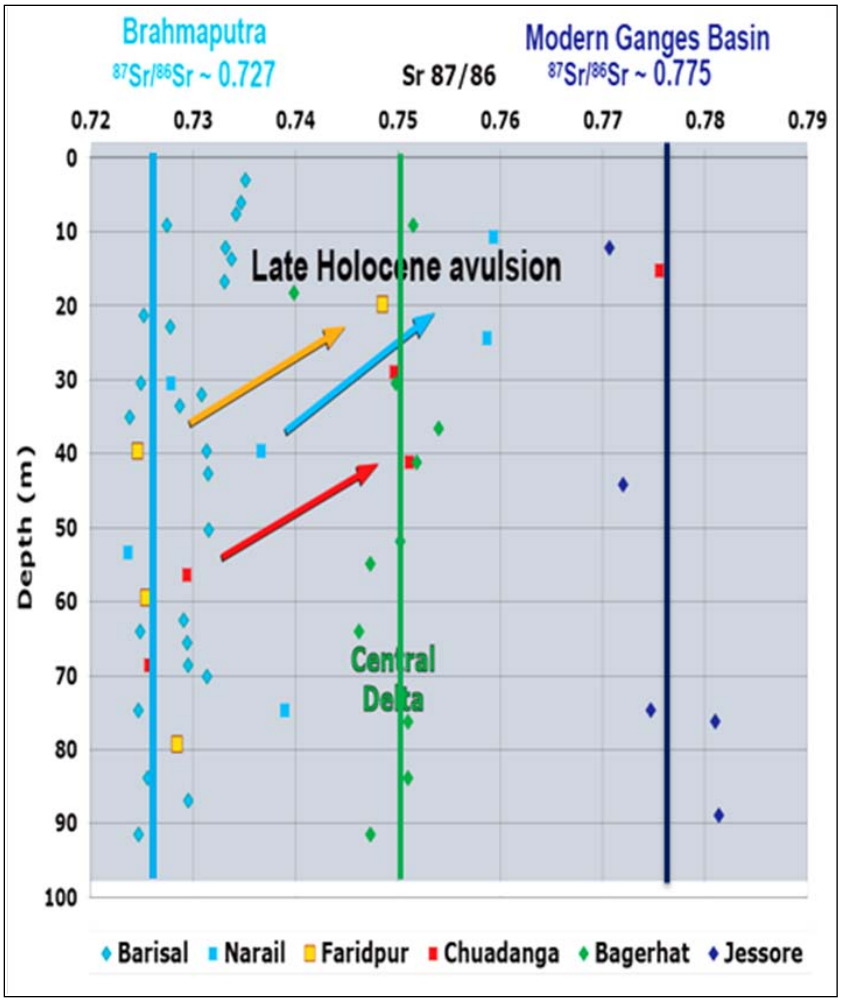

Figure 4.10. Showing the sudden increase of isotopic ratios in the few G-B delta boreholes indicating the late Holocene avulsion of the Ganges and Brahmaputra River. The blue and violet lines represent the average isotopic ratio of the Brahmaputra (Tibet) and the modern Ganges (Higher Himalaya) sediment respectively. The green line symbolizes the isotopic ratios of one of the central boreholes, which is considered as a mixing between the two-river systems.

CHAPTER V

Conclusions

The Ganges and Brahmaputra rivers, which drain the High Himalayas, Lesser Himalayas, Tibetan Sedimentary Series and Tibetan plateau, have transported the major portion of late Quaternary sediments to the Ganges - Brahmaputra (G-B) delta, Bangladesh. These major lithologic groups also have distinctive Sr concentrations and isotopic ratios, which are used in this study to understand the river avulsion and abandonment, and shifting provenance sources for the G-B delta.

From previous studies it was found that sediments derived from the Tibetan Plateau and Tethyan Himalaya have high (> 200 ppm) Sr concentrations with very low Sr isotopic ratios (0.71 – 0.73). In contrast, Lesser Himalayan sediments usually have very low (<70 ppm) Sr concentrations with a high isotopic ratios (> 0.81). High Himalayan sediments also have low (70-100 ppm) Sr concentrations but an intermediate isotopic ratios (0.73 – 0.78). These contrasting Sr concentrations and isotopic ratios were used in this study to differentiate the Ganges sediment input from the Brahmaputra during the Late Quaternary period in the Ganges-Brahmaputra delta. Sediment eroded from the Brahmaputra watershed is less radiogenic than Ganges sediments because of significant sediment contribution from the Tibetan and Tethyan Himalayan lithologies. Brahmaputra sediments typically have $^{87}Sr/^{86}Sr$ values in the range of 0.72 to 0.74, while Ganges sediments have significantly higher $^{87}Sr/^{86}Sr$ values approaching 0.80, because of sediment flux dominated by more radiogenic Lesser and High Himalayan lithologies. The Brahmaputra sediment input in the G-B delta can also be differentiated by its high Sr concentrations (> 140 ppm) compared to the Ganges sediment (<110 ppm). The third river that might bring a significant

amount of sediment into the G-B delta is the Tista, which is presently a western tributary of the Brahmaputra. However, its sediment shows higher $^{87}Sr/^{86}Sr$ values than Brahmaputra (> 0.80).

Although the traditional approach for provenance studies in the Himalayan region involves only Sr isotopic ratio, Sr concentrations of the borehole sediments in this research also proven an effective provenance indicator in the G-B delta. A histogram of all Sr concentration data from the G-B delta borehole sediment shows that the Late Quaternary deposit in the G-B delta had derived from all the major source areas in the Himalayas and Tibet. Moreover, the presence of only Brahmaputra sediments in the Late Pleistocene sequence found in the present study also implies that a large portion of the Late Quaternary G-B delta sediment have their provenances in the Tibetan Plateau and the in the Tethyan Himalaya. However, the Higher Himalaya, which is a common sediment source of both Ganges and Brahmaputra River, seems to supply the bulk of the sediment during both the Holocene and Pleistocene. Therefore, this research concludes that the dominant sources of the Late Quaternary sediments in the G-B delta are from Himalayan signature (mostly High Himalaya) from Ganges and partially the Brahmaputra, with Tibetan sources exclusively from the Brahmaputra basin. The lower Sr concentrations and isotopic values found in three boreholes in Sylhet basin also indicate considerable local input from Shillong Plateau from the N-E direction.

This research also attempts a provenance analysis by comparing both the Sr concentrations and the isotopic ratios of the studied borehole sediments with their various end members sources. It was found that the 90 m Holocene sequence in the Jessore borehole is almost entirely of High Himalayan origin. However, samples collected from the Chuadanga and Narail boreholes show both the Himalayan (High Himalayan and Tethyan Himalayan) and Tibetan signature. The higher isotopic ratios in the upper part of the stratigraphic sequence in Narail and Chuadanga indicate a greater sediment input from Himalayan sequences starting from the Early Holocene. The sediment samples, which have intermediate Sr isotopic ratios between Higher

Himalayan and Tibetan end member sources, most probably represent a period in between Late Pleistocene and Early Holocene where there is an equal share of sediment from both Himalaya and Tibet.

The Sr concentrations and isotopic ratios of the borehole sediments at different depths from all over the G-B delta supports a model where the Brahmaputra was the principal source of sediment deposited in the delta during the Late Pleistocene. Sr concentrations of Pleistocene sediments from 12 boreholes across the G-B delta are well above 150 ppm and are presumed to indicate transport by the Brahmaputra alone. In contrast, the Sr concentrations of Holocene sediments collected from the same boreholes show an increasing Sr concentration from west to east where Ganges only dominated the extreme western part of the delta. Based on the variation in Sr concentrations of the Holocene sediments from west to east, the G-B delta thus can be divided into three deltaic zones - the Eastern, Central and Western delta. The Eastern delta contains Ganges input during Holocene alone, with a maximum Sr concentration of 119 ppm. The Central delta is a mixing zone between the Ganges and Brahmaputra Holocene sediments that record abrupt changes in river position presumably avulsion. In the western delta, Holocene sediments were deposited mostly by the Brahmaputra and contain high Sr concentrations greater than 158 ppm.

The Sr concentrations and isotopic values of the borehole sediments collected from all over the G-B delta also reveal a compelling story of river avulsion during the late Quaternary. The Pleistocene Brahmaputra sediment found in the extreme east as far as Kustia and Chuadanga on one hand and the Ganges dominated Holocene sequence in the western and central G-B delta on the other hand does indicate several phases of the Brahmaputra and Ganges River avulsion from west to east throughout the Late Quaternary period. Based on the Sr concentration and isotopic ratio values at different boreholes in these three zones and the river dynamics, the late Quaternary depositional history of the G-B delta is also proposed in this study. During the Late

Pleistocene, Ganges River had less influence on the sedimentation in the G-B delta as reflected by the high Sr concentration values of the Pleistocene sediments. Most sediment deposited before the Holocene therefore derived from the Brahmaputra, which built the delta from Chuadanga to the west to Raipur to the east. However, the patterns of sediment dispersal in the G-B delta have changed from the Early Holocene, when the Ganges river system started to contribute a large portion of sediment to the western and central delta. This application of river avulsion to distinguish the fluvial-deltaic sequence provides a first-order understanding of the deltaic evolution and stratigraphic sequence development in the high - sediment yield, tectonically active G-B delta.

REFERENCES CITED

Ahmad, S.M., Babu, G.A., Padmakumari, V.M., Dayal, A.M., Sukhija, B.S., and Nagabhushanam, P., 2005. Sr, Nd isotopic evidence of terrigenous flux variations in the Bay of Bengal: Implications of monsoons during the last~34,000 years. Geophysical Research Letters, vol. 32.

Allison, M. A., Khan, S. R., Goodbred, S. L., and Kuehl, S. A., 2003. Stratigraphic evolution of the late Holocene Ganges-Brahmaputra lower delta plain. Sedimentary Geology, vol. 155, p. 317-342.

Biswas, S., Coutand, I., Grujic, D., Hager, C., Stöckli, D. and Grasemann, B., 2007. Exhumation and uplift of the Shillong plateau and its influence on the eastern Himalayas: New constraints from apatite and zircon (U-Th-[Sm])/He and apatite fission track analyses. Tectonics, vol. 26, doi:10.1029/2007TC002125.

Burg, J.P., Davy, P., Nievergelt, P., Oberli, F., Seward, D., Diao, Z., and Meier, M., 1997. Exhumation during crustal folding in the Namche Barwa syntaxis: Terra Nova, vol. 9, p. 53–56, doi: 10.1111/j.1365-3121.1997.tb00001.x.

Célérier, J.T., Harrison, M., Webb, A.G. and Yin, A., 2009. The Kumaun and Garwhal Lesser Himalaya, India: Part 1. Structure and stratigraphy. GSA Bulletin, September/October 2009; vol. 121, no. 9/10; p. 1262–1280.

Chinese Research Institute of Surveying and Mapping, China Mountaineering Association, 1990. Namjagbarwa Mountaineering Map (1:50,000), ISBN 7-5031-0538-0.).

Clift, P. D., Giosan, L., Blusztajn, J., Campbell, I. H., Allen, C., Pringle, M., Tabrez, A. R., Danish, M., Rabbani, M. M., Alizai, A., Carter, A., and Luckge, A., 2008. Holocene erosion of the Lesser Himalaya triggered by intensified summer monsoon. Geology, pages 79-82.

Debon, F., LeFort, P., Sheppard, S.M.F., Sonet, J., 1986. The four plutonic belts of the Transhimalaya - Himalaya: a chemical, mineralogical, isotopic and chronological synthesis along a Tibet-Nepal section. J. Petrol., Vol. 27, pp. 219 -250.

Derry, L. A. and France-Lanord, C., 1997. Himalayan weathering and erosion fluxes: Climate and tectonic controls. Global Tectonics and Climate Change, pages 289-312.

Finnegan, N.J., Hallet, B., Montgomery, D.R., Zeitler, P.K., Stone, J.O., Anders, A.M and Yuping, L., 2008. Coupling of rock uplift and river incision in the Namche Barwa–Gyala Peri massif, Tibet. GSA Bulletin, January/February 2008, vol. 120, p. 142–155; doi:10.1130/B26224.1

Galy, A., and France-Lanord, C., 2001. Higher erosion rates in the Himalaya: Geochemical constraints on riverine fluxes. Geology, vol. 29, p. 23-26.

Galy, A., Lanord, C.F. and Derry, L.A., 1999. The strontium isotopic budget of Himalayan Rivers in Nepal and Bangladesh. Geochimica et Cosmochimica Acta, Vol. 63, No. 13/14, pp. 1905–1925

Garzanti, E., Vezzoli, G., Ando, S., France-Lanord, C., Singh, S.K. and Foster, G., 2004. Sand petrology and focused erosion in collision orogens: The Brahmaputra case. Earth and Planetary Science Letters, vol. 220, p. 157–174, doi:10.1016/S0012-821X(04)00035-4.

Goodbred, S.L., 2003. Response of the Ganges dispersal system to climate change: A source-to sink view since the last interstade. Sedimentary Geology, vol. 162, p. 83–104.

Goodbred, S. L., Kuehl, S. A., Steckler, M. S., and Sarker, M. H., 2003. Controls on facies distribution and stratigraphic preservation in the Ganges-Brahmaputra delta sequence. Sedimentary Geology, vol.155, p. 301- 316.

Goodbred, S. L. and Kuehl, S. A., 2000 (b). The significance of large sediment supply, active tectonism, and eustasy on margin sequence development: Late Quaternary stratigraphy and evolution of the Ganges-Brahmaputra delta. Sedimentary Geology, 133:227-248.

Heroy,D.C., Kuehl, S.A., Goodbred, S.L., 2003. Mineralogy of the Ganges and Brahmaputra Rivers: implications for river switching and Late Quaternary climate change. Sedimentary Geology, vol. 155, pp. 343 -359.

Islam, M.R., Begum, S.F., Yamaguchi, Y., Ogawa, K., 1999. The Ganges and Brahmaputra rivers in Bangladesh: basin denudation and sedimentation. Hydrol. Proces, vol. 13, pp. 2907-2923.

Kuehl, S. A., Allison, M. A., Goodbred, S. L., and Kudrass, H., 2005. River Deltas - Concepts, Models, and Examples: The Ganges-Brahmaputra Delta. SEPM Special Publication, vol. 83.

Lanord, C.F., Derry, L., Michard, A., 1993. Evolution of the Himalaya since Miocene time: isotopic and sedimentologic evidence from the Bengal Fan. Himalayan Tectonics, Geol. Soc. Lond Spec. Publ. 74, pp. 603-621.

McArthur, J. M., et al., 2004. Natural organic matter in sedimentary basins and its relation to arsenic in anoxic groundwater: The example of West Bengal and its worldwide implications. Appl. Geochem., 19, 1255– 1293, doi:10.1016/j.apgeochem.2004.02.001.

McArthur, J. M., Ravenscroft, P., Banerjee, D. M., Milsom, J., Hudson-Edwards, K. A., Sengupta, S., Bristow, C., Sarkar, A., Tonkin, S. and Purohit, R., 2008. How paleosols influence groundwater flow and arsenic pollution: A model from the Bengal Basin and its worldwide implication. Water Resources Research, vol. 44, w11411, doi:10.1029/2007WR006552, 2008.

Milliman, J.D., Syvitski, P.M., 1992. Geomorphic/Tectonic control of sediment discharge to the ocean: the importance of small mountainous rivers. J. Geol. 100, p. 525-544.

Najman, Y., 2006. The detrital record of orogenesis: A review of approaches and techniques used in the Himalayan sedimentary basins. Earth Science Reviews, 74:1-72.

Pate, R.D., 2008. Stratigraphic and facies analysis: Bengal basin, Bangladesh. Unpublished M.S. Thesis, Vanderbilt University, Nashville, TN, USA.

Segall, M.P., Kuehl, S.A., 1992. Sedimentary processes on the Bengal continental shelf as revealed by clay-size mineralogy. Continental Shelf Research, vol. 12 (4), 517– 541.

Singh, S.K., Rai, S.K., and Krishnaswami, S., 2008. Sr and Nd isotopes in river sediments from the Ganga Basin: Sediment provenance and hotspots of physical erosion: Journal of Geophysical Research, v. 113.

Singh, S. K., Kumar, A., and France-Lanord, C., 2006. Sr and $^{87}Sr/^{86}Sr$ in waters and sediments of the Brahmaputra river system: Silicate weathering, CO2 consumption and Sr ux. Chemical Geology, vol. 234:308-320.

Singh, S.K., Lanord, C.F., 2002. Tracing the distribution of erosion in the Brahmaputra watershed from isotopic compositions of stream sediments. Earth and Planetary Science Letters, vol. 202, pp. 645-662.

Stewart, R.J., Hallet, B., Zeitler, P.K., Malloy, M.A., Allen, C.M. and Trippett, D., 2008. Brahmaputra sediment flux dominated by highly localized rapid erosion from the easternmost Himalaya. Geology, vol. 36, pp. 711-714, doi: 10.1130/G24890A.1.

Tibari, B., Pik, R., France-Lanord, C., Carnigan, J.,and Lave, J., 2005. Extreme uplift and erosion rates in eastern Himalayas (Siang-Brahmaputra Basin) revealed by detrital (U-Th)/He thermochronology. Eos (Transactions, American Geophysical Union), v. 85, Fall Meeting Supplement, Abstract T23C–0574.

Verosub, K. L. and Roberts, A. P., 1995. Environmental magnetism, past, present, and future. Journal of Geophysical Research, 100:2175-2192.

Wasson, R. J., 2003. A sediment budget for the Ganga–Brahmaputra Catchment. Current Science, vol. 84, no. 8.

Zeitler, P.K., Malloy, M.A., Kutney, M.P., Idleman, B.D., Liu, Y., Kidd, W.S., and Booth, A.L., 2006. Geochronological evidence for the tectonic and topographic evolution of SE Tibet: Eos (Transactions, American Geophysical Union), v. 87, Abstract T23B–0480.

APPENDIX

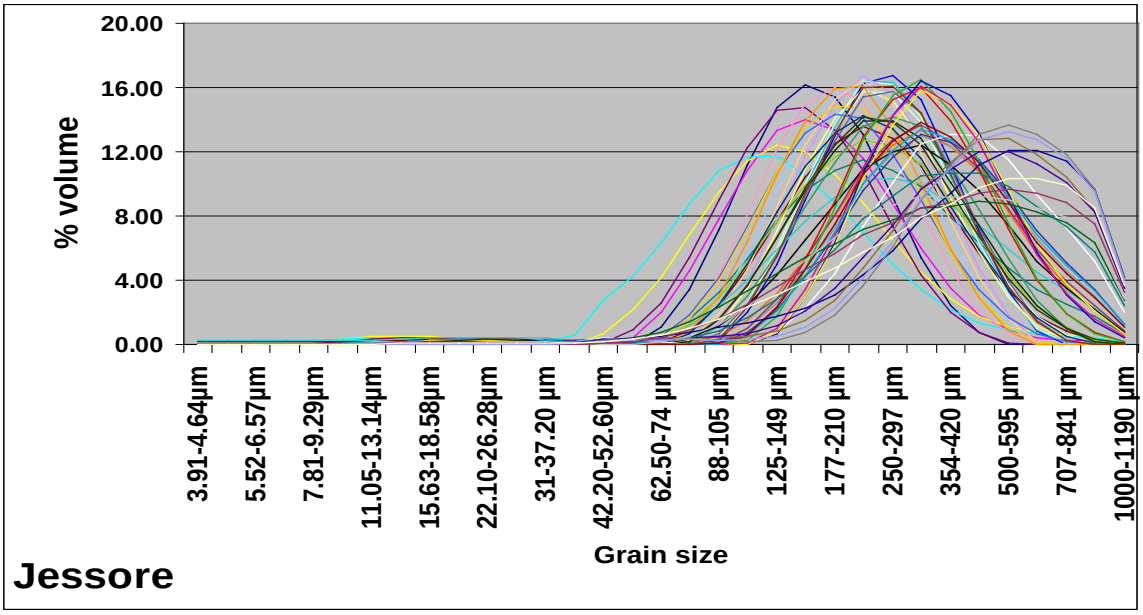
20.00
16.00
12.00
8.00
4.00
0.00
% volume
3.91-4.64µm
5.52-6.57µm
7.81-9.29µm
11.05-13.14µm
15.63-18.58µm
22.10-26.28µm
31-37.20 µm
42.20-52.60µm
62.50-74 µm
88-105 µm
125-149 µm
177-210 µm
250-297 µm
354-420 µm
500-595 µm
707-841 µm
1000-1190 µm
Grain size
Jessore

(a)

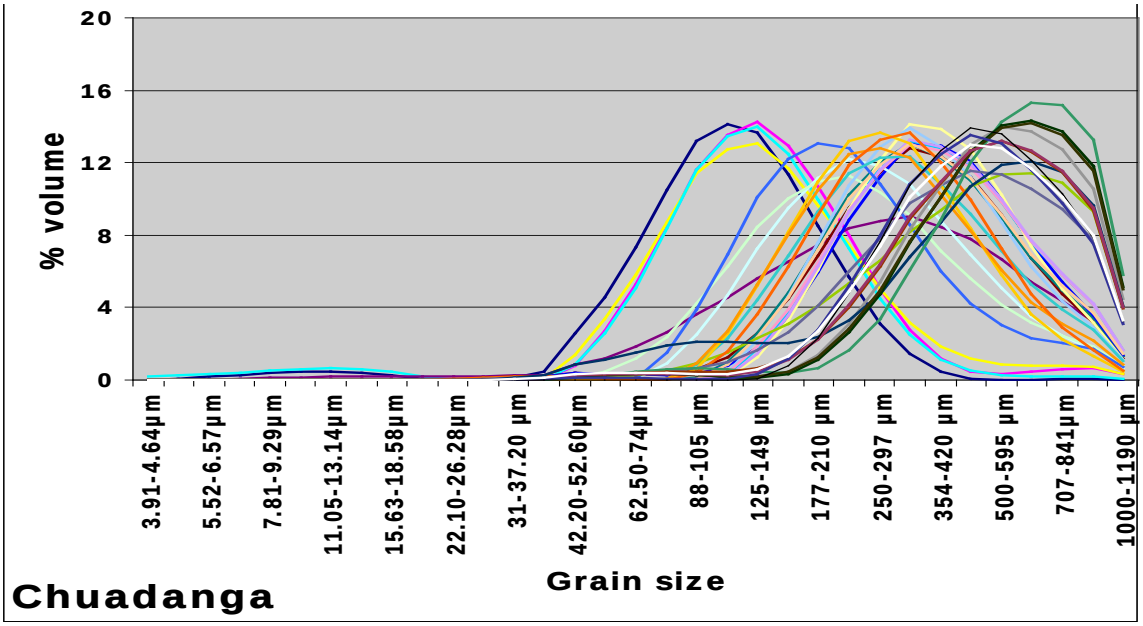
20
16
12
8
4
0
% volume
3.91-4.64µm
5.52-6.57µm
7.81-9.29µm
11.05-13.14µm
15.63-18.58µm
22.10-26.28µm
31-37.20 µm
42.20-52.60µm
62.50-74µm
88-105 µm
125-149 µm
177-210 µm
250-297 µm
354-420 µm
500-595 µm
707-841µm
1000-1190 µm
Grain size
Chuadanga

(b)

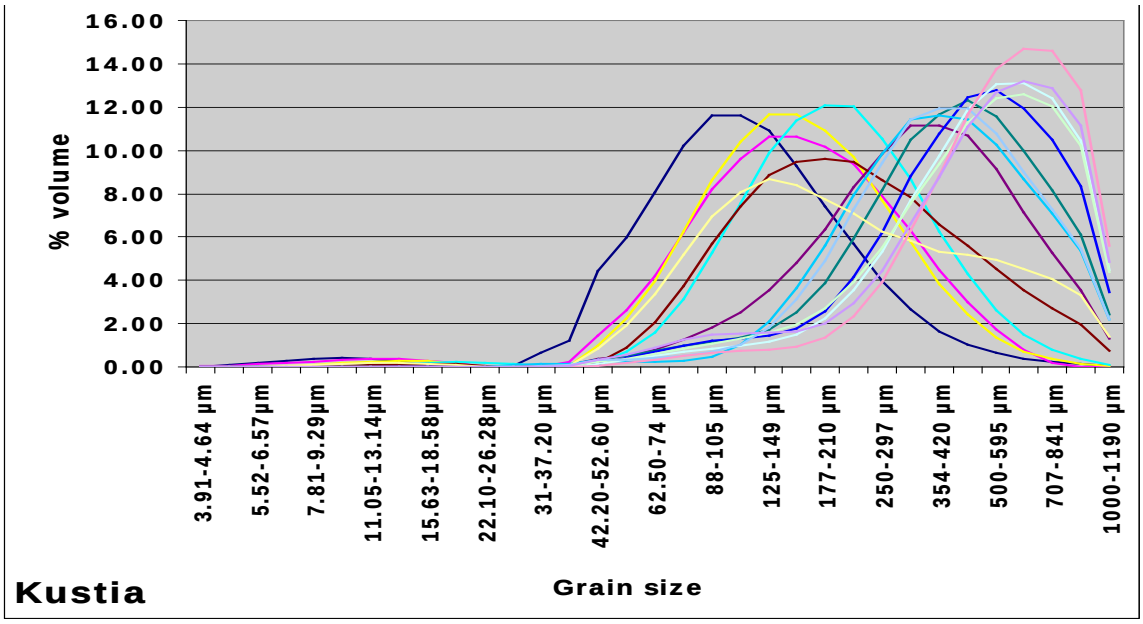

(c)

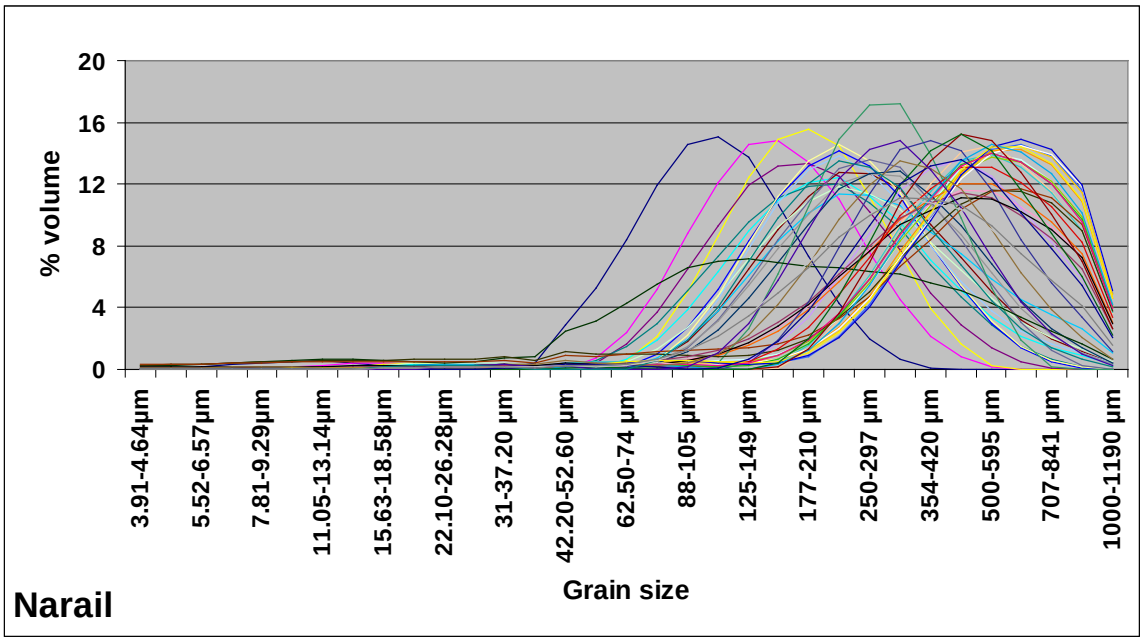

(d)

Figure B.1: Sand fractions from the four boreholes showing the modal distributions.

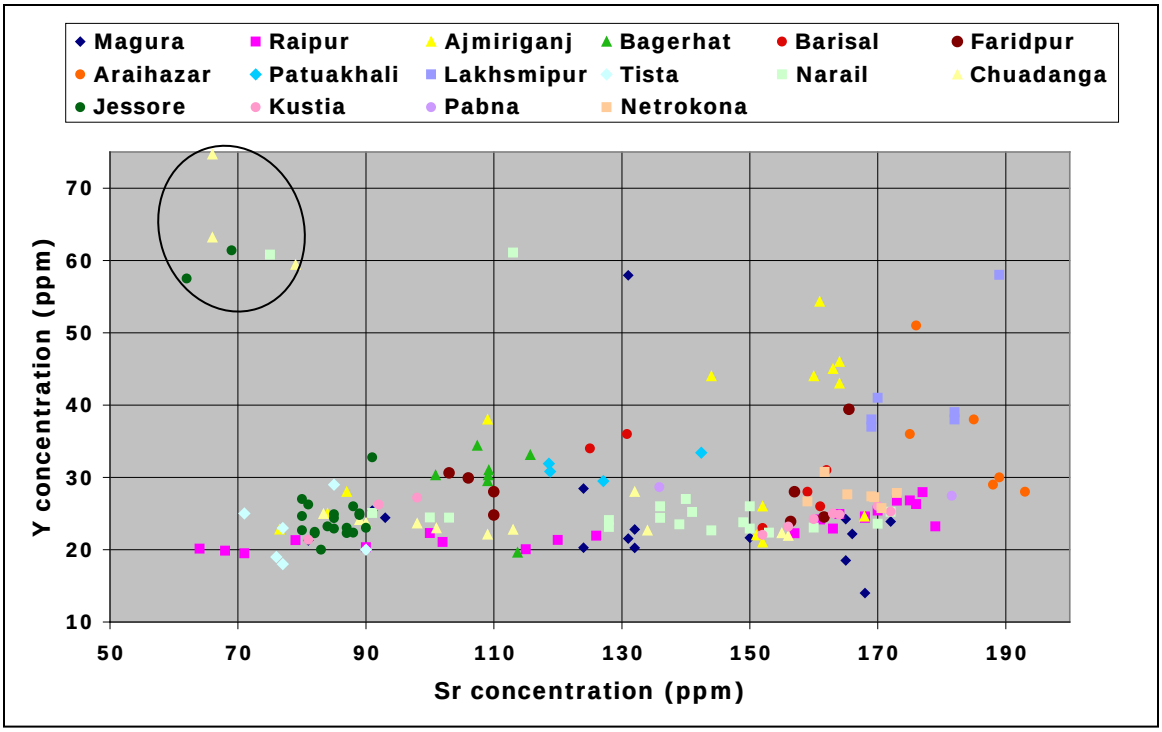

Figure B.2: A plot of Sr vs. Y concentrations from the all available Bangle Basin borehole.

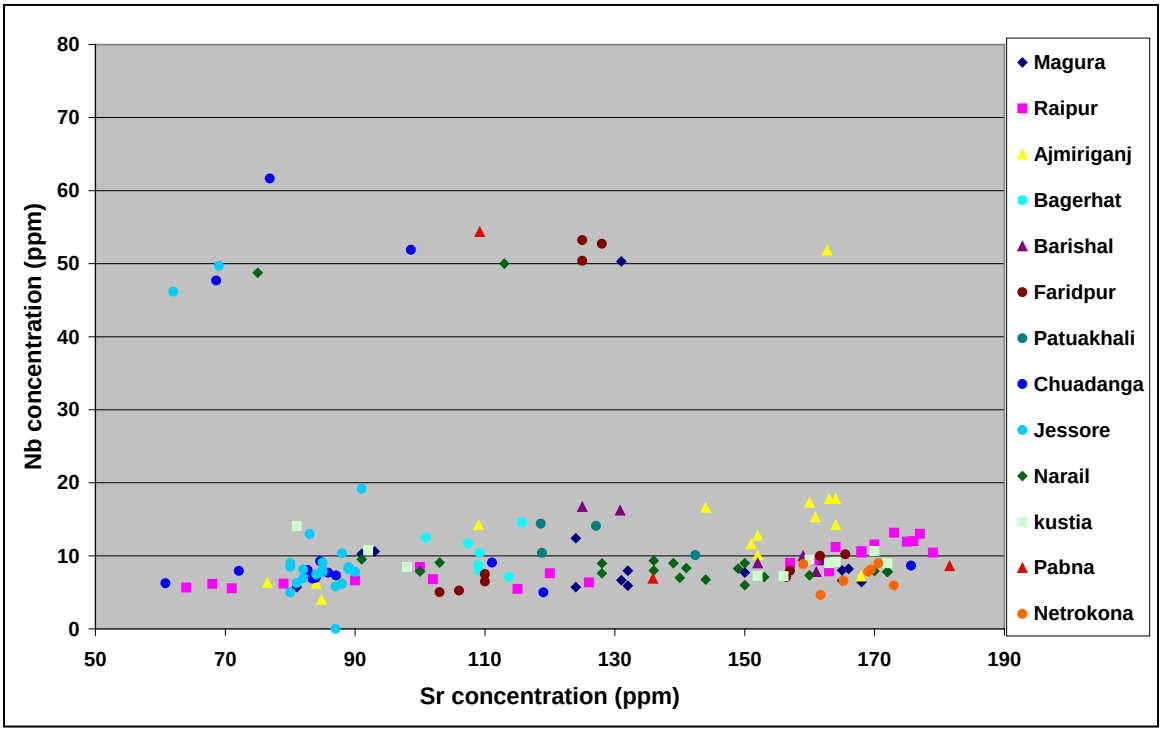

Figure B.3: A plot of Sr vs. Nb concentrations from the all available Bangle Basin borehole.

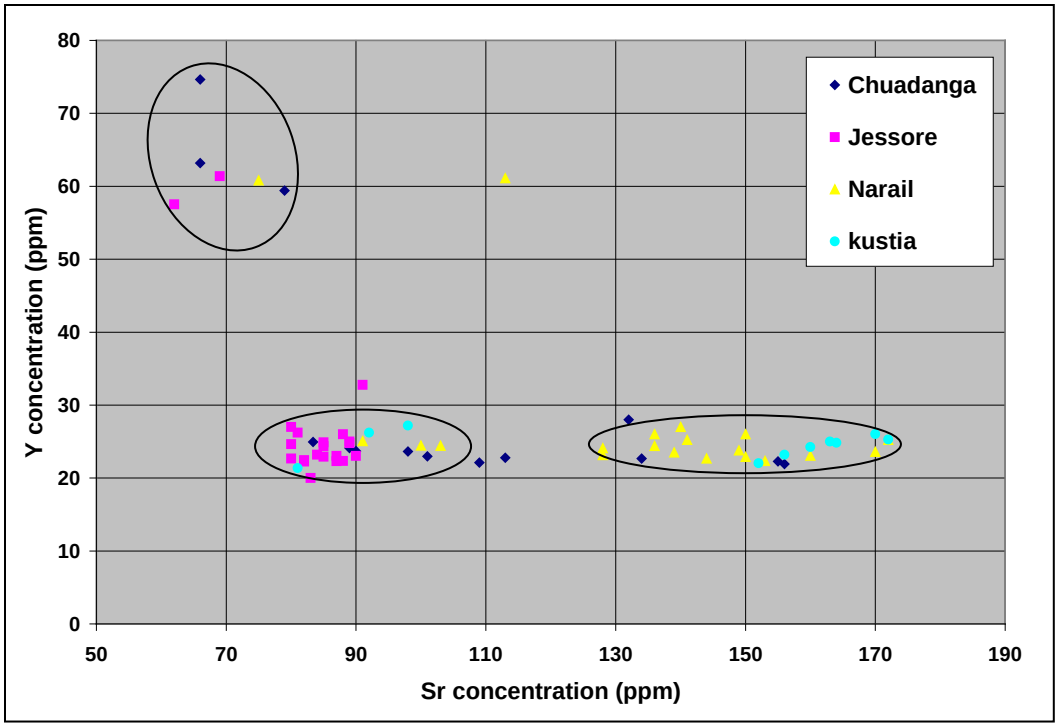

Figure B.4: A plot of Sr vs. Y concentrations from the boreholes used in the present research showing three distinct groups.

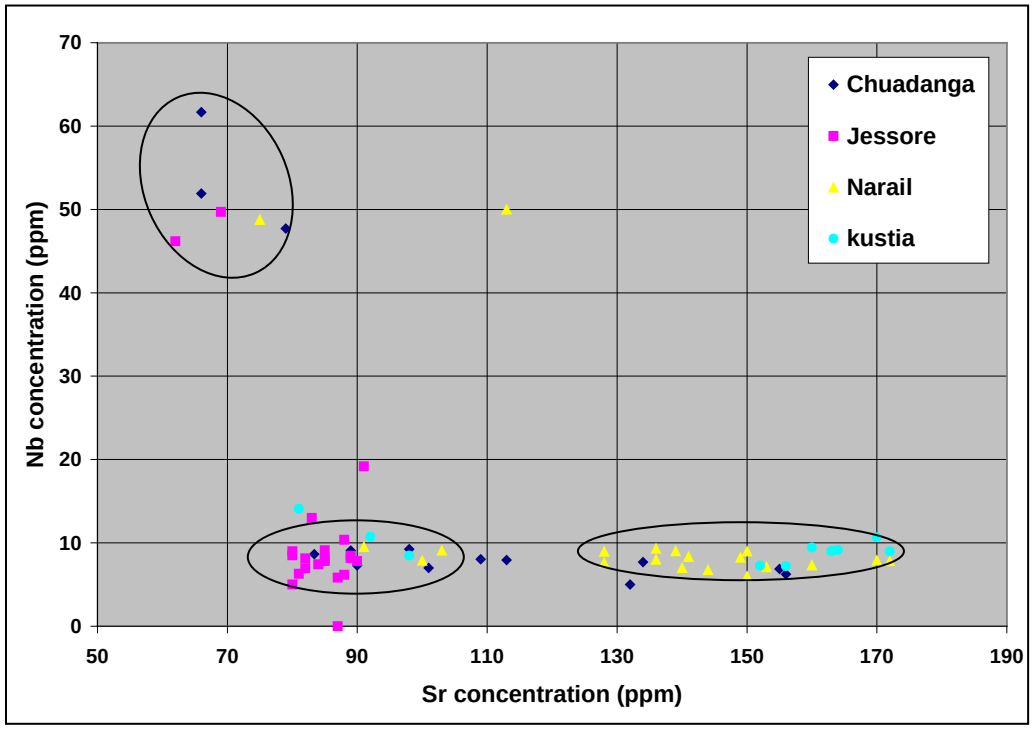

Figure B.5: A plot of Sr vs. Nb concentrations from the boreholes used in the present research showing three distinct groups.

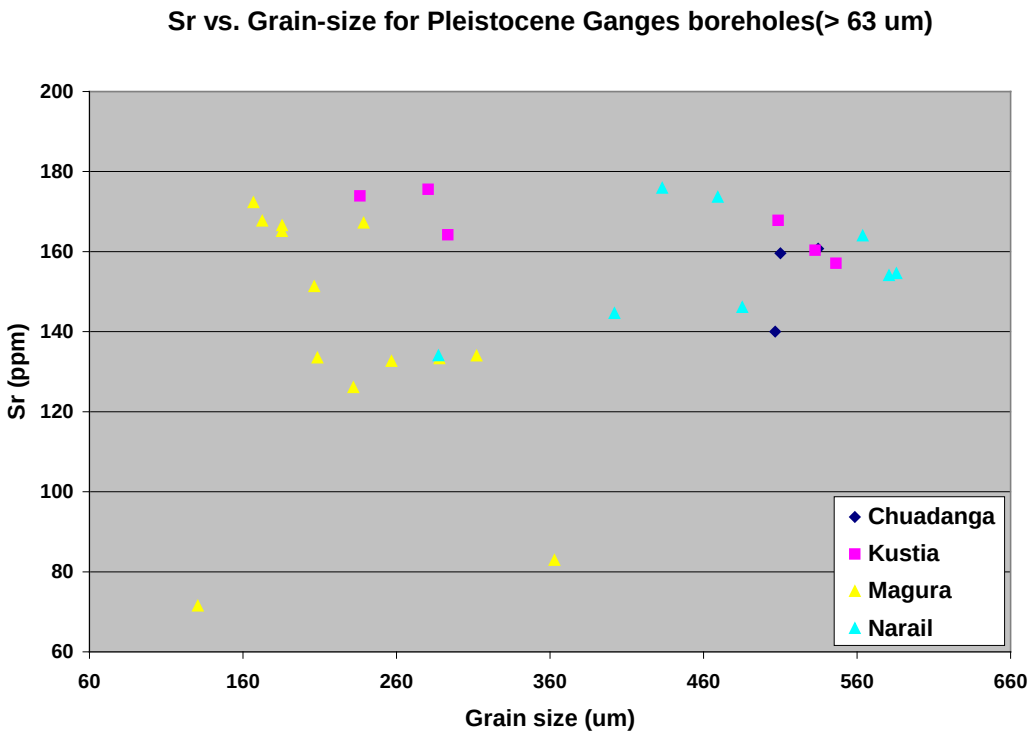

Figure B.6: Grain size vs. Sr concentrations for the Pleistocene samples from the boreholes used in the present research.

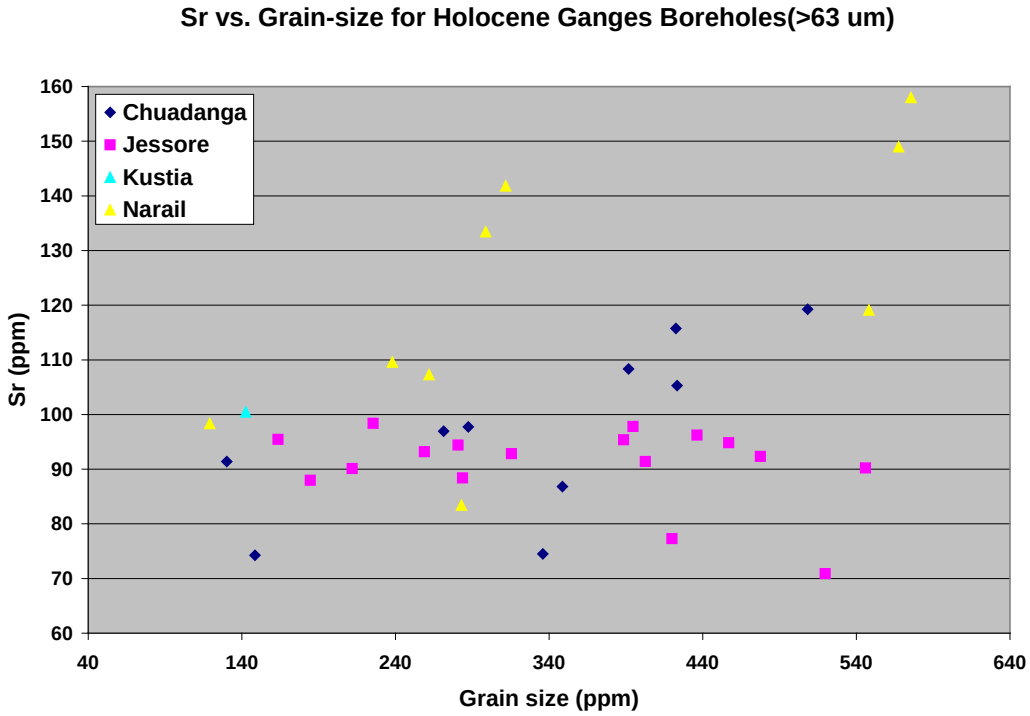

Figure B.7: Grain size vs. Sr concentrations for the Holocene samples from the boreholes used in the present research.